

Data-driven risk mitigation and flexibility enhancement in perishable supply chain networks

Mohammad Mehdi Tahmouresi, Javad Behnamian ^{*}

Industrial Engineering Department, Faculty of Engineering, Bu-Ali Sina University, Hamedan, Iran

ARTICLE INFO

Keywords:

Resilient supply chain
Robust data-driven planning
Just-in-time manufacturing
Perishable goods
NSGA-II

ABSTRACT

Supply chains operating in dynamic, high-risk environments need mechanisms that preserve economic efficiency while strengthening resilience to disruptions. This study develops an integrated, data-driven framework for four-echelon supply chains (suppliers, manufacturers, distributors, retailers) that explicitly models route disruptions, transportation capacity limits, product perishability, and production and storage constraints for finished goods and raw materials, together with uncertain customer demand. By considering these factors simultaneously, the model shows that production and storage limits critically influence system performance and that demand uncertainty increases operational complexity and cost. To this end, the study formulates a bi-objective, linearized Mixed-Integer Programming (MIP) model that minimizes (*i*) overall operational cost and (*ii*) network inflexibility, measured by the number of critical points and allocation counts, thereby capturing trade-offs among efficiency, risk mitigation, and flexibility. To address practical Just-In-Time (JIT) shortcomings under uncertainty, the model allows multi-sourcing (distributors can source from multiple manufacturers; manufacturers can procure from multiple suppliers), enhancing robustness relative to conventional configurations. Uncertainty is treated with a data-driven Distributionally Robust Optimization (DRO) approach. The model is solved with exact CPLEX routines via the augmented ϵ -constraint method for moderate-sized instances, and with the Non-dominated Sorting Genetic Algorithm II (NSGA-II) for large instances. Performance is benchmarked against a Multi-Objective Particle Swarm Optimization (MOPSO) comparator. Computational experiments—conducted on datasets supplied by Khoshgavar Company (soft-drink production and distribution)—demonstrate that NSGA-II yields superior Pareto fronts (proximity, dispersion, objective attainment) while enabling tractable solutions at practical scales. Results further indicate that risk-averse strategies, although costlier in the short term, materially improve long-term resilience by lowering disruption impact and systemic exposure. The integrated framework advances theory by bridging resilience, JIT, and robust data-driven planning, and offers actionable managerial guidance for industries handling perishable goods (e.g., food and cold-chain pharmaceuticals), including strategies to balance cost and flexibility under uncertainty.

1. Introduction

Designing an efficient supply chain network (SCN) plays a critical role in achieving coordinated operations, reduced inventory levels, improved capacity utilization, shortened lead times, and enhanced customer service levels [1]. When SCNs handle perishable goods, additional challenges emerge: limited coordination among members, insufficient demand information across stages, complex order and inventory management, and strict product-expiration constraints. These issues can lead to severe consequences—delivery delays may cause shortages, inventory accumulation, and spoilage that reduce market

share and customer satisfaction, while premature deliveries can cause product deterioration before consumption [2]. Just-In-Time (JIT) systems aim to deliver materials and components at the right place and time while minimizing waste and operational costs, and therefore are attractive for improving efficiency [3]. However, applying JIT without adequate consideration of environmental uncertainty increases vulnerability to disruptive events. Resilience—defined as the ability of a system to absorb shocks, recover, and return to an acceptable state after disruption—is thus essential to sustain SCN performance under stress [4]. In practice, supply-chain risks stem from two main sources: operational risks arising from inherent supply-demand coordination

* Corresponding author.

E-mail address: Behnamian@basu.ac.ir (J. Behnamian).

variability, and disruption risks resulting from external shocks such as natural disasters or economic instability [5]. Ignoring these risks can significantly undermine supply-chain reliability and performance, whereas a resilient SCN can absorb disturbances and maintain acceptable service levels [6].

Perishable-product supply chains face acute exposure due to rapid spoilage and limited shelf life. They therefore contend with multiple interacting risks, including intrinsic operational risks, disruption-related risks, demand uncertainty, and capacity constraints in transportation, storage, and production [7]. To represent real-world conditions more faithfully, this study treats these interdependent factors simultaneously and develops an integrated model that improves coordination among supply-chain components while aiming to reduce operational cost and waste. Methodologically, the model embeds JIT principles to optimize inventory levels and minimize waste, but supplements them with resilience mechanisms to mitigate JIT's sensitivity to disruptions [8]. Demand uncertainty is addressed with a data-driven, distributionally robust optimization approach so that decisions remain reliable under ambiguous demand distributions. The network is modeled as a geographically dispersed, four-echelon system (suppliers, manufacturers, distributors, retailers) with explicit modeling of route disruptions and operational constraints, including predefined delivery dates and penalty costs for deviations; route disruptions are represented via a probabilistic component while retailer demand is treated through data-driven robust techniques. The principal contribution of this research is an explicit analysis of the trade-off among cost, flexibility, and resilience. The formulation is a bi-objective linear programming problem that minimizes total operational cost and network inflexibility, thereby highlighting the interaction between short-term cost increases—treated as necessary investments for risk mitigation—and the long-term benefits of improved sustainability and resilience. Unlike many prior studies that analyze these dimensions separately, the integrated approach here yields richer managerial insights; for example, the model's capacity to simulate diverse disruption scenarios supports prescriptive guidance for inventory policies, contingency planning, and route selection under uncertainty. The solution approach follows established practices in linear and robust optimization. Implementation uses standard tools. For moderate-sized instances, the enhanced ϵ -constraint method implemented in GAMS with exact CPLEX routines is applied; for large-scale instances, the Non-dominated Sorting Genetic Algorithm II (NSGA-II) is used and benchmarked against a Multi-Objective Particle Swarm Optimization (MOPSO). Computational results validate the efficiency and applicability of the proposed method in realistic supply-chain environments. Key innovations of the study include: (i) the simultaneous evaluation of resilience and JIT strategies within a single, integrated framework; (ii) explicit modeling of variable vehicle capacities and product perishability; (iii) combined treatment of demand uncertainty and route disruptions using data-driven robust and probabilistic methods; and (iv) a detailed trade-off analysis between cost minimization and network flexibility that produces actionable managerial recommendations.

The remainder of this paper is organized as follows: The second section will present a review of the most related studies on SC design. The third section will describe the problem and its assumptions and evaluate the mathematical model of how to deal with the issues of multi-objectiveness and uncertainty. The fourth section will describe the

algorithm. The fifth section will provide and analyze the numerical results. Finally, the sixth section will present the conclusion and future suggestions.

2. Literature review

Vali-Siar and Roghanian [9] addressed the green and resilient supply chain network design (SCND) problem. They considered possible disruptions in suppliers and manufacturing sites as well as transportation scheduling and its environmental impacts. To formulate the problem, they developed a bi-objective mixed integer stochastic programming model with the objective functions of minimizing the total costs and total carbon emissions. They used the Augmented Epsilon Constraint (AEC) method to solve the problem. Mousavi et al. [10] proposed a multi-objective mathematical model for designing a green and resilient cement SCN aimed at increasing the SC demand and simultaneously mitigating the costs imposed by CO₂ emissions. They utilized the scenario-based method to solve the model. Sadeghi et al. [11] modeled the problem of sustainable and resilient planning of a four-echelon SCN. To this aim, they developed a multi-objective mathematical model with the objectives of minimizing the costs, maximizing the social and environmental scores of the suppliers for the sustainability of the SC, and minimizing the delivery delays. They employed the AEC and LP metrics to ensure the balance of the objectives. Mehralian et al. [12] developed the Supply Chain Operations Reference (SCOR) model and identified important factors in three components: agile supply, agile manufacturing, and agile distribution. Using Fuzzy TOPSIS in each component, they ranked the factors. Having analyzed the data, they concluded that the speed of delivery directly increases the speed of the SC. Moreover, cost mitigation inside and outside the organization affects the total product costs and can enhance SC responsiveness. To develop the SC agility model based on the SCOR model, Zarenezhad et al. [13] proposed a conceptual model for the agility of each of the SC processes, namely supply, manufacturing, and distribution using the fuzzy TOPSIS mathematical algorithm and Friedman's statistical test. Azad et al. [14] proposed a resilient supply chain network (RESCND) model under the risk of facility disruptions and transportation links with the aim of determining the optimal location, types of distribution centers (DCs), and the best program for the allocation of customers to these centers. They employed the Benders decomposition method to solve their model. Garcia-Herreros et al. [15] proposed a RESCND model under disruption considerations with the aim of minimizing the total investment and distribution costs and taking into account complete facility disruption risks. In addition, they applied a two-stage stochastic programming formulation to counter threats. Nooraei and Parast [16] proposed a time-dependent RESCND model under partial facility disruptions to manage SC disruptions and evaluated several resilience strategies, including multiple sourcing and providing backup facilities. Ghavamifar et al. [17] proposed a multi-objective RESCND model under disruption risks in a competitive environment. Taking into account complete facility disruptions, they adopted resilience strategies and used the Benders Composition method to solve their model. Diabat et al. [18] proposed a four-echelon RESCND model consisting of suppliers, fixed and mobile warehouses, DCs, and customers, considering the reliability and disruption risks of facilities and routes between them. They applied robust stochastic programming along with multi-criteria

decision-making (MCDM) to minimize dispatch time and delivery cost during a disaster. Yan and Ji [19] addressed the RESCND, considering simultaneous uncertainty and disruptions. They applied planning under uncertainty to manage disruptions and risks in a multi-echelon SC to meet customer demands and achieve the minimum cost simultaneously. They also utilized the Lagrange relaxation method to simplify the solution process. Dehghani et al. [20] proposed a bi-objective model for RESCND under uncertainty and multiple disruptions to minimize total cost and inflexibility. They also used the ϵ -constraint method and two-stage stochastic programming to deal with the objective functions. Jafari-Nodoushan et al. [21] developed a three-objective model for RESCND, which uses a robust approach to minimize costs, enhance resilience, and ensure product pricing during a disaster.

Khalili et al. [22] developed a two-stage scenario-based mixed stochastic-pessimistic programming model for designing a three-echelon gasoline supply chain (GSC) that jointly accounted for sustainability (costs, CO₂ emissions, social impacts) and resilience (design quality, proactive and reactive capabilities) under operational and disruption risks. The first stage determined network configuration and pre-disruption mitigation options, while the second stage optimized distribution, network reconfiguration, and capacity restoration; the model handled imprecise parameters and scenario planning and introduced an augmented-CVaR metric to better manage high-impact, low-probability disruptions. Karanam et al. [23] formulated a multi-objective MILP for perishable food supply chain networks (PFSCN) that minimized total cost and total time under static and dynamic conditions while incorporating realistic perishability and network constraints. They proposed a modified NSGA-II (MNSGA-II) for static scenarios and developed a heuristic using degree-of-disruption and node-threshold measures to estimate ripple-effect impacts in dynamic scenarios, quantifying performance metrics such as service level, robustness, resilience, and efficiency. Bakhshi Sasi et al. [24] investigated disruption mitigation in global food supply chains (GFSC) facing supply and transportation interruptions, including sequences of multiple disruptions, and formulated the initial and post-disruption plans as MILP models. They proposed a novel heuristic that rapidly revised the ideal plan after disruptions, capable of handling different disruption types and successive events, with design choices aimed at fast reoptimization under time constraints. Ansari et al. [25] formulated a multi-stage stochastic programming model for sustainable humanitarian relief that optimized location, allocation, and inventory across pre-, during-, and post-disaster stages while balancing environmental, social, and economic objectives. They solved the multi-objective model using an augmented epsilon-constraint method, employed MCDM supplier ranking enhanced by machine-learning algorithms, and integrated data-driven techniques to determine stage-wise priorities (environmental emphasis in stages 1 and 3, social focus in stage 2). Hosseini Shekarabi et al. [26] developed an extended robust optimization model for sustainable and resilient supply-chain network design for perishable products that jointly considered budget allocation between SCN design and external investments, supplier selection, and transfer-based retailer resilience. They proposed an axis-shift robust method combined with an enhanced p-robust framework, integrated an AI-based neural-network disruption predictor, and used multi-cut Benders decomposition with goal programming to handle multiple objectives (profitability, environmental sustainability, job creation). Tabatabaei [27] developed a multi-objective mixed-integer programming model for sustainable supply-chain network design that integrated risk management, resilient

multimodal transportation, and production strategy to maximize profit, minimize transportation time, and reduce environmental impact. He/she introduced a goal-programming solution approach and a hybrid solver combining local search with machine-learning predictive models to handle the MOMIP complexity and validated the model with real data from the Iranian chemicals industry. Vázquez-Serrano et al. [28] developed a hybrid optimization–discrete-event simulation framework for inventory control and pricing of perishable products in multi-echelon supply chains, deriving unit-level critical selling prices and handling multi-product, multi-period uncertainty. Their model combined optimization for inventory cost minimization with simulation to capture operational variability, producing analytic formulas for break-even prices both with and without operational costs. Lingkon et al. [29] developed an integrated location–inventory–routing (LIR) model for perishable goods that simultaneously optimized product freshness, total cost, and carbon footprint. They implemented a multi-objective metaheuristic using YALMIP for solution handling and performed sensitivity analysis to examine factors such as vehicle speed and its trade-off between emissions and cost. Rezki and Mansouri [30] developed a mixed-integer linear programming model for strategic supply-chain network design that jointly considered economic cost minimization, environmental emissions, and disruption risk costs to capture trade-offs among efficiency, sustainability, and resilience. They integrated a Belief Bayesian Network (BBN) to predict and quantify disruption risk probabilities and applied belief-propagation analysis to identify the most sensitive risk factors and subfactors influencing the network. Recently, Hosseini Shekarabi et al. [31] systematically reviewed supply-chain resilience literature (294 articles, 2000–2024) using bibliometric and network analyses framed by dynamic capabilities to map the field. They applied keyword co-occurrence and research-focus parallelship networks to identify three research clusters: optimization for resilience, technology adoption for resilience, and resilience strategies for disruption and risk management.

Table 1 presents a comparison of the reviewed studies on the JIT and resilient SC of perishable products. It is evident from the table that while these studies effectively address individual facets of supply chain management (such as demand uncertainty, resilience, or JIT) using either exact or metaheuristic methods, none have simultaneously integrated all three dimensions—in particular, data-driven planning, resilience, and JIT into one comprehensive mathematical framework. The study under discussion makes several notable contributions.

- The research integrates data-driven robust optimization, scenario-based stochastic programming, the augmented ϵ -constraint method, and NSGA-II in a single four-echelon perishable supply chain framework (suppliers, manufacturers, distributors, retailers). Unlike prior work that treats resilience, JIT, demand uncertainty, or data-driven planning separately, this unified model captures route disruptions, transport capacity, production/storage limits, perishability, and uncertain retailer demand, enabling explicit trade-off analysis between efficiency, risk mitigation, and network flexibility.
- The paper uses a hybrid uncertainty scheme: scenario-based stochastic programming for route and high-impact, low-probability disruptions, and a data-driven robust demand set for ambiguous or limited demand data. This preserves scenario fidelity for disruptions while providing distribution-free protection for demand.
- Operational realism and perishability focus: the model enforces production and storage constraints, vehicle capacity, perishability

Table 1
A summary of the literature review.

Ref.	Objective functions	JIT	Resiliency	Demand	Model & Solution method	Descriptions
Vali-Siar & Roghanian [9]	Minimize cost; Minimize carbon emissions	No	Yes	Stochastic	Bi-objective stochastic MIP; solved by AEC	Green resilient SCND (bi-objective)
Mousavi et al. [10]	Increase demand; Minimize CO ₂ cost	No	Yes	Stochastic	Multi-objective model with scenario generation	Green cement SCN (multi-objective)
Sadeghi et al. [11]	Minimize cost; Maximize social/env. scores; Minimize delays	No	Yes	Stochastic	Multi-objective MIP; AEC + LP metrics	Sustainable resilient 4-echelon
Mehralian et al. [12]	Rank agility factors; Assess delivery speed & cost	No	Agility focus	Deterministic	Fuzzy TOPSIS (MCDM)	SCOR agility factors (ranking)
Zarenezhad et al. [13]	Develop SCOR-based agility; Rank factors	No	Agility focus	Deterministic	Fuzzy TOPSIS + Friedman test	Conceptual SC agility model
Azad et al. [14]	Optimal DC locations; Customer allocation	No	Yes	Stochastic (disruptions)	Resilient SCND MIP; Benders decomposition	RESCND with facility/link disruptions
Garcia-Herreros et al. [15]	Minimize investment & distribution cost	No	Yes	Stochastic	Two-stage stochastic programming	RESCND under complete facility disruption
Nooraie & Parast [16]	Minimize SC costs; Evaluate resilience strategies	No	Yes	Stochastic	Time-dependent MIP; stochastic programming	Time-dependent RESCND (partial disruptions)
Ghavamifar et al. [17]	Minimize costs (multi objectives)	No	Yes	Stochastic	Multi-objective resilient MIP; Benders composition	Multi-objective RESCND in competition
Diabat et al. [18]	Minimize dispatch time; Minimize disaster delivery cost	No	Yes	Robust/Stochastic	Robust stochastic multi-objective model; MCDM	Four-echelon RESCND (robust)
Yan & Ji [19]	Minimize cost while meeting demand	No	Yes	Stochastic	Planning-under-uncertainty MIP; Lagrangian relaxation	RESCND with simultaneous uncertainty
Dehghani et al. [20]	Minimize total cost; Minimize inflexibility	No	Yes	Stochastic	Bi-objective stochastic MIP; ϵ -constraint + two-stage	Bi-objective RESCND (inflexibility)
Jafari-Nodoushan et al. [21]	Minimize cost; Enhance resilience; Ensure pricing	No	Yes	Robust/Stochastic	Robust multi-objective MIP; robust programming	Three-objective robust RESCND
Khalili et al. [22]	Sustainability & resilience metrics	No	Yes	Stochastic + Possibilistic	Two-stage stochastic-pessimistic programming; augmented CVaR	Gasoline GSC (three-echelon, two-stage)
Karanam et al. [23]	Minimize cost & time; Improve service & resilience	No	Yes	Static & Dynamic	Multi-objective MILP; MNSGA-II (static) + heuristic (dynamic)	PFSCN for perishables
Bakhshi Sasi et al. [24]	Rapid recovery; Maintain service	No	Yes	Stochastic (successive disruptions)	MILP pre/post; fast reoptimization heuristic	GFSC disruption mitigation (rapid replan)
Ansari et al. [25]	Balance environmental, social, economic objectives by stage	No	Yes	Stochastic (multi-stage)	Multi-stage stochastic programming; augmented ϵ -constraint; MCDM + ML	Multi-stage stochastic for humanitarian relief
Hosseini Shekarabi et al. [26]	Profitability; Sustainability; Job creation; Resilience	No	Yes	Robust/Stochastic	Robust MIP (axis-shift, p-robust); multi-cut Benders; neural predictor	Perishable SCN with AI predictor
Tabatabaei [27]	Maximize profit; Minimize transport time; Reduce env. impact	No	Yes	Deterministic/validated	Multi-objective MIP; goal programming + hybrid solver	MOMIP for sustainable SCN (chemical industry case)
Vázquez Serrano et al. [28]	Minimize inventory cost; Derive critical prices	No	Yes	Stochastic (multi-period)	Optimization + Discrete Event Simulation hybrid	Perishable pricing/inventory with simulation
Lingkong et al. [29]	Optimize freshness; Minimize cost & emissions	No	Yes	Stochastic	Integrated LIR MIP; multi-objective metaheuristic (YALMIP)	Integrated LIR for perishables
Rezki & Mansouri [30]	Minimize economic & env. costs; Minimize disruption risk costs	No	Yes	Stochastic (BBN risk)	MILP + Belief Bayesian Network; belief propagation	Strategic SCN with BBN for disruption risk
This study	Minimize operational cost; Minimize network inflexibility	Yes (integrated with multi sourcing)	Yes (route disruptions, multi sourcing, robust planning)	Stochastic (uncertain customer demand)	Bi objective MIP+ ϵ -constraint; NSGA II and MOPSO	integrated four echelon perishable SCN with route disruptions

dynamics, and JIT timing, avoiding unconstrained relocations and producing a tighter, actionable feasible region for perishable logistics (multi-sourcing, procurement, routing, inventory rules).

- Explicit bi-objective trade-off between cost and flexibility: minimizing operational cost and network inflexibility together makes short-term resilience costs and long-term benefits directly comparable, shifting emphasis to operational inflexibility as a decision objective.

- Hybrid solution strategy balancing exactness and scalability: augmented ϵ -constraint in GAMS supplies exact Pareto anchors for moderate instances; NSGA-II (benchmarked with MOPSO) handles large, high-dimensional problems, combining solution quality with computational tractability.
- Differentiated modeling choices that change feasible tactical responses. Compared with Dehghani et al. [20] and Jafari Nodoushan et al. [21], who focused on network level robust/stochastic design, this study addresses an operational coordination problem:

coordinating production, routing and delivery under strict JIT timing and mixed uncertainties for perishables. Modeling heterogeneous uncertainties with scenario disruptions plus a data driven demand uncertainty set, enforcing vehicle capacity and perishability, and disallowing arbitrary material relocation produce different feasible responses and more actionable operational trade offs than those in prior network design studies.

- Empirical benchmarking and managerial implications: computational experiments show that risk-averse configurations (multi-sourcing, buffers, conservative replenishment) raise short-term costs but substantially reduce systemic disruption exposure, offering concrete guidance on inventory policy, contingency planning, and route selection for perishables.
- Fills a documented gap: while many studies address subsets (stochastic/robust design, JIT, perishability, simulation, fast reoptimization), no existing work simultaneously integrates route disruptions, transport capacity, production/storage constraints, perishability, JIT mechanics, multi-echelon structure, and mixed (scenario + data-driven) uncertainty for perishable supply chains; this study fills that gap.
- Methodological extension and validation: the work combines exact multi-objective techniques (augmented ϵ -constraint) with population-based metaheuristics (NSGA-II vs. MOPSO), incorporates data-driven robust set construction and AI-based prediction where applicable, and synthesizes methods across the literature to deliver validated, scalable solutions.

3. Problem statement and modeling

This study proposed a multi-period four-echelon perishable product SC problem consisting of raw material suppliers, manufacturers, distributors, and retailers at the first to fourth echelons, respectively. In the first echelon, the raw materials are supplied and transported to the warehouse according to the manufacturers' demand. Next, they are converted into products by manufacturers according to the demand of the distributors. Then, the defective products are separated, and the distributors' demand is responded to. After storing the products, the distributors supply the retailers' uncertain demand on a daily basis. Each product sent in each period has a one-period delivery date, and a penalty

will be imposed on the model if it is sent later than the delivery time. In this problem, the goal is to minimize the costs of construction, purchase of raw materials, manufacturing, storage, transportation, distribution, backlog sale, destruction of defective products, and excess transportation, thereby reducing the inflexibility of the problem against possible disruptions. The assumptions of the research are as follows.

- The model comprises four echelons: suppliers, manufacturers, distributors, and retailers.
- The demand of retailers in each period is uncertain.
- Disruptions occur on routes among different echelons.
- Disruption scenarios have a constant occurrence rate and occur independently.
- All products have a fixed and specific life cycle, which will perish after the end of their life cycle.
- There is a limited manufacturing capacity.
- The raw materials and products have a limited storage capacity.
- Vehicles have a limited weight capacity and number.
- The unanswered demand is considered a backlog sale and is transferred to the next period.
- Disruptions occur on routes.
- Means of transportation can only move between two echelons in each period.
- The delivery date of all orders is one period.
- The potential location of all facilities is already known.
- The products cannot be stored in the supplier's warehouse; rather, they are transported to a lower echelon in the same period.
- The products or raw materials cannot be transported among the members of the same echelon of the SC.

A schematic view of the problem is shown in Fig. 1.

3.1. Mathematical modeling

The mathematical model proposed in this study is a linear programming model with an uncertain demand parameter. Considering the presence of uncertain parameters in the model, a data-driven planning approach was used to model the problem. Indices, parameters, decision

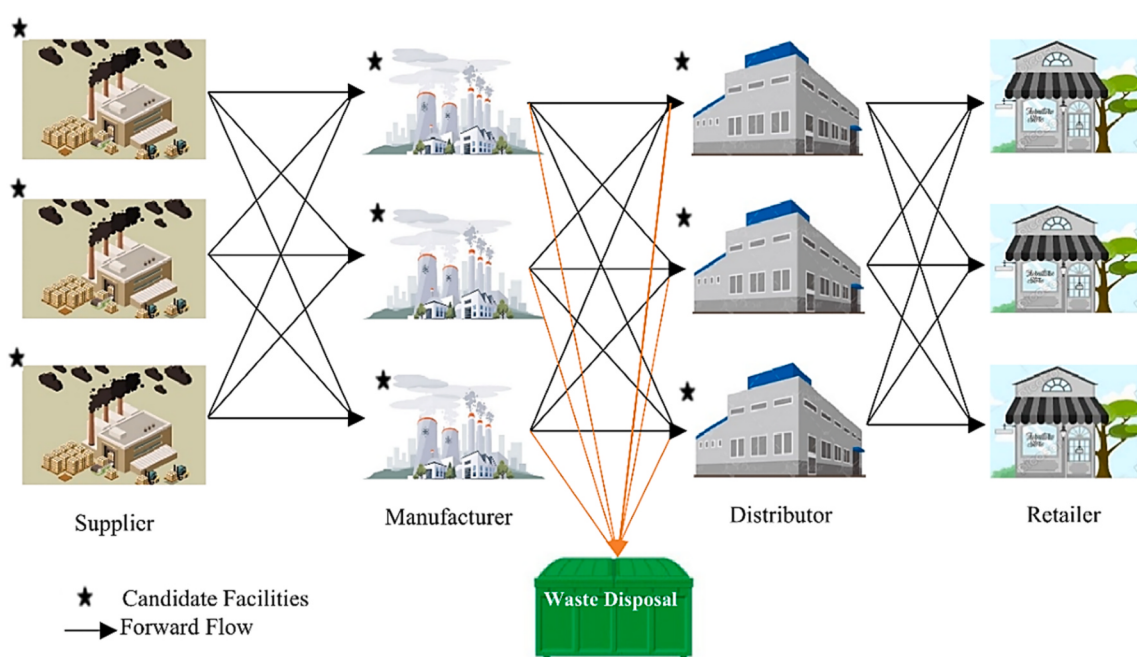


Fig. 1. The proposed robust and resilient SC configuration.

variables, objective function, and constraints are given below.

Indices	
S	Index of suppliers
M	Index of manufacturers
W	Index of distributors
C	Index of retailers
I	Index of raw materials
P	Index of products
R_1	Index of routes between suppliers and manufacturers
R_2	Index of routes between manufacturers and distributors
R_3	Index of routes between distributors and retailers
K	Index of vehicles
T	Index of periods
O	Index of disruption scenarios
U	Index of demand uncertainty scenarios
Parameters	
φ_1	Penalty factor for supplier construction
φ_2	Penalty factor for manufacturer construction r
φ_3	Penalty factor for distributor construction
μ_1	Penalty factor for allocation of manufacturer m to supplier s
μ_2	Penalty factor for allocation of distributor w to manufacturer m
μ_3	Penalty factor for allocation of retailer c to distributor w
θ_1	Penalty factor for supplier criticality
θ_2	Penalty factor for manufacturer criticality
θ_3	Penalty factor for distributor criticality
ω_{smr_1to}	If a disruption o occurs between supplier s and manufacturer m on route r during period t , its value will be 1. If a disruption o occurs between manufacturer m and distributor w on route r during period t , its value will be 1. If a disruption o occurs between manufacturer m and retailer c on the route during period t , its value will be 1.
η_{mwr_2to}	The transport capacity of raw material i from supplier s during period t
λ_{wcr3to}	The transport capacity of product p from manufacturer m during period t
$CapT_{ist}$	The transport capacity of product p from distributor w during period t
$CapT_{pmt}$	The percentage decrease of transport capacity of raw material i from supplier s during period t under scenarios o and u
RT_{istou}	The percentage decrease of transport capacity of product p from manufacturer m during period t under scenarios o and u
RT_{pmtou}	The percentage decrease of transport capacity of product p from distributor w during period t under scenarios o and u
EX_p	The life cycle of product p
Re_{pmtou}	The percentage of manufacturing waste of product p in factory m during period t under scenarios o and u
RP_{pmtou}	The percentage decrease of nominal manufacturing capacity of product p in factory m during period t under scenarios o and u
RH_{mtou}	The percentage decrease of storage capacity of factory m during period t under scenarios o and u
RH_{wtou}	The percentage decrease of storage capacity of distributor w during period t under scenarios o and u
$CapP_{pmt}$	Nominal manufacturing capacity of product p in factory m
$CapH_{mt}$	Nominal storage capacity in factor m
$CapH_{wt}$	Nominal storage capacity in DC w
δ_ip	Conversion factor of raw materials i into product p
De_{pctou}	Uncertain demand for product p by retailer c during period t under scenarios o and u
τ_{sou}	Threshold limit of criticality of supplier s under scenarios o and u
τ_{mou}	Threshold limit of criticality of manufacturer m under scenarios o and u
τ_{wou}	Threshold limit of criticality of DC w under scenarios o and u
π_o	Probability of occurrence of scenario o
β_u	Probability of occurrence of scenario u
EC_s	The construction cost of supplier s
EC_m	The construction cost of manufacturer m
EC_w	The construction cost of DC w
$TC1_{r_1ktou}$	Cost of supplying goods from supplier s to manufacturer m by vehicle k during period t under scenarios o and u
$TC2_{r_2ktou}$	Cost of supplying goods from manufacturer m to DC w by vehicle k during period t under scenarios o and u
DC_{r_3ktou}	Cost of distributing products from DC w to retailer c by vehicle k during period t under scenarios o and u
ds_{smr_1}	Distance between supplier s and manufacturer m from route r
dm_{mwr_2}	Distance between manufacturer m and DC w from route r
dw_{wcr_3}	Distance between DC w and retailer c from route r
PC_{pmtou}	Manufacturing cost per unit of product p in factory m during period t under scenarios o and u

(continued on next column)

(continued)

Indices	
PCE_{pmtou}	Destruction cost per unit of defective product p manufactured in factory m during period t under scenarios o and u
ECE_{pwtou}	Destruction cost per unit of spoiled product p in DC w during period t under scenarios o and u
SC_{pctou}	Cost per unit of backlog sales during period t under scenarios o and u
$HC1_{intou}$	Maintenance cost per unit of raw material i for manufacturer m during period t under scenarios o and u
$HC2_{pwtou}$	Maintenance cost per unit of product p in DC w during period t under scenarios o and u
VC_{istou}	Transportation cost per unit of excess capacity raw material i from supplier s during period t under scenarios o and u
VC_{pmtou}	Transportation cost per unit of excess capacity product p from manufacturer m during period t under scenarios o and u
VC_{pwtou}	Transportation cost per unit of excess capacity product p from warehouse w during period t under scenarios o and u
B_i	Buying cost per unit of raw material i
$CapV_k$	Maximum weight capacity of vehicle k
$CapZ_k$	Maximum number capacity of vehicle k
ρ_p	The capacity of each package of product p
BM	Large positive number
Decision variables	
OS_s	A binary variable whose value equals one if supplier s is constructed
OM_m	A binary variable whose value equals one if manufacturer m is constructed
OW_w	A binary variable whose value equals one if warehouse w is constructed
SM_{ismr_1ktou}	If raw material i is supplied by factory m from supplier s and from route r_1 by vehicle k during period t and under scenarios o and u , its value will be 1.
MW_{pmwr_2ktou}	If product p is supplied by DC w from manufacturer m and from route r_2 by vehicle k during period t and under scenarios o and u , its value will be 1.
WC_{pwcr_3ktou}	If the demand for product p is supplied by retailer c from DC w and from route r_3 by vehicle k during period t and under scenarios o and u , its value will equal 1.
CM_m	If the activities of manufacturer m exceed the threshold, its value will be 1.
CW_w	If the activities of warehouse w exceed the threshold, its value will be 1.
CS_s	If the activities of supplier s exceed the threshold, its value will be 1.
$TA1_{ipsmr_1ktou}$	Amount of raw material i of product p transported from supplier s to manufacturer m from route r_1 and by vehicle k during period t and under scenarios o and u
$TA2_{pmwr_2ktou}$	Amount of product p transported from manufacturer m to DC w from route r_2 and by vehicle k during period t and under scenarios o and u
$TA3_{pwcr_3ktou}$	Amount of product p transported from DC w to retailer c through route r_3 and by vehicle k during period t and under scenarios o and u
ETC_{istou}	Amount of increased transport capacity of raw material i from supplier s during period t and under scenarios o and u
ETC_{pmtou}	Amount of increased transport capacity of product p from manufacturer m during period t and under scenarios o and u
ETC_{pwtou}	Amount of increased transport capacity of product p from DC w during period t and under scenarios o and u
TAE_{pwtou}	Amount of expired product p in DC w during period t and under scenarios o and u
x_{pwcr_3ktou}	Amount of product p distributed in its life cycle from DC w and route r_3 by vehicle k during period t and under scenario o
PA_{pmtou}	Amount of product p manufactured in factory m during period t and under scenarios o and u
$PFE_{ipsmtou}$	Amount of raw material i of product p purchased from supplier s by factory m during period t and under scenarios o and u
$IL1_{ipmtou}$	Inventory level of raw material i of product p in factory m during period t and under scenarios o and u
$IL2_{pwtou}$	Inventory level of product p in DC w during period t and under scenarios o and u
LS_{pctou}	Lost sales of product p by retailer c during period t and under scenarios o and u
Z_{pmwr_2ktou}	Number of packages of product p transported between manufacturer m and DC w from route r_2 by vehicle k during period t and scenarios o and u
$TFOC$	Facility construction cost
TBC_{ou}	Cost of buying raw materials under scenarios o and u
TTC_{ou}	Supply cost under scenarios o and u
TDC_{ou}	Distribution cost under scenarios o and u
TOC_{ou}	Manufacturing cost under scenarios o and u
THC_{ou}	Maintenance cost under scenarios o and u

(continued on next page)

(continued)

Indices	
$TSHC_{ou}$	Lost sales cost under scenarios o and u
$TECC_{ou}$	Excess transportation cost under scenarios o and u
η_u	A binary variable
v_u	A binary variable
ζ_u	A binary variable
$mincost$	Minimum cost
TN	Minimum complexity

Based on [20], the model of the study is as follows:

$$\begin{aligned} \text{Min } z_1 &= mincost \\ &= TFOC + TBC + TOC + TTC + TDC + THC + TECC \end{aligned} \quad (1)$$

$$\begin{aligned} \text{Min } z_2 &= TN \\ &= \sum_s \varphi_1 OS_s + \sum_m \varphi_2 OM_m + \sum_w \varphi_3 OW_w + \sum_s \theta_1 CS_s + \sum_m \theta_2 CM_m \\ &\quad + \sum_w \theta_3 CW_w + \sum_{ismr_1 kt} \mu_1 SM_{ismr_1 kt} + \sum_{mwr_2 kp} \mu_2 MW_{mwr_2 kt} \\ &\quad + \sum_{wcr_3 kt} \mu_3 WC_{wcr_3 kt} \end{aligned} \quad (2)$$

$$TFOC = \sum_s EC_s OS_s + \sum_m EC_m OM_m + \sum_w EC_w OW_w \quad (3)$$

$$TBC = \sum_{ismr_1 kt} TA1_{ismr_1 kt} B_i \quad (4)$$

$$TCC = \sum_{ismr_1 kt} TA1_{ismr_1 kt} TC1_{r_1 kt} ds_{smr_1} + \sum_{mwr_2 kt} TA2_{mwr_2 kt} TC2_{r_2 kt} dm_{mwr_2} \quad (5)$$

$$TDC = \sum_{pwcr_3 kt} TA3_{pwcr_3 kt} DC_{r_3 kt} dw_{wcr_3} \quad (6)$$

$$TOC = \sum_{pmt} PC_{pmt} PA_{pmt} + \sum_{pmt} PCe_{pmt} RPA_{pmt} \quad (7)$$

$$TSHC = \sum_{pct} SC_{pct} LS_{pct} \quad (8)$$

$$THC = \sum_{ipmt} HC1_{ipmt} IL1_{ipmt} + \sum_{pwt} HC2_{pwt} IL2_{pwt} + \sum_{pwt} ECe_{pwt} TAE_{pwt} \quad (9)$$

$$TECC = \sum_{ist} VC1_{ist} ETC1_{ist} + \sum_{pmt} VC2_{pmt} ETC2_{pmt} + \sum_{pwt} VC3_{pwt} ETC3_{pwt} \quad (10)$$

s.t. :

$$\sum_{r_1 k} SM_{ismr_1 kt} \leq 1 \quad \forall i, s, m, t \quad (11)$$

$$\sum_{r_2 k} MW_{mwr_2 kt} \leq 1 \quad \forall p, m, w, t \quad (12)$$

$$\sum_{r_3 k} WC_{wcr_3 kt} \leq 1 \quad \forall w, c, t \quad (13)$$

$$\sum_{ik} SM_{ismr_1 kt} \leq OS_s(1 - \omega_{smr_1 t}) \quad \forall s, m, r_1, t \quad (14)$$

$$\sum_{ik} SM_{ismr_1 kt} \leq OM_m(1 - \omega_{smr_1 t}) \quad \forall s, m, r_1, t \quad (15)$$

$$\sum_{pk} MW_{pmwr_2 kt} \leq OM_m(1 - \eta_{mwr_2 t}) \quad \forall m, w, r_2, t \quad (16)$$

$$\sum_{pk} MW_{pmwr_2 kt} \leq OW_w(1 - \eta_{mwr_2 t}) \quad \forall m, w, r_2, t \quad (17)$$

$$\sum_k WC_{wcr_3 kt} \leq OW_w(1 - \lambda_{wcr_3 t}) \quad \forall w, c, r_3, t \quad (18)$$

$$\sum_{pmr_1 k} TA1_{pmr_1 kt} \leq (1 - RT1_{ist}) CapT_{ist} OS_s + ETC_{ist} \quad \forall i, s, t \quad (19)$$

$$ETC_{ist} \leq RT1_{ist} CapT_{ist} OS_s \quad \forall i, s, t \quad (20)$$

$$\sum_{wr_2 k} TA2_{pmwr_2 kt} \leq (1 - RT2_{pmt}) CapT_{pmt} OM_m + ETC_{pmt} \quad \forall p, m, t \quad (21)$$

$$ETC_{pmt} \leq RT2_{pmt} CapT_{pmt} OM_m \quad \forall p, m, t \quad (22)$$

$$\sum_{cr_3 k} TA3_{pwcr_3 kt} \leq (1 - RT3_{pwt}) CapT_{pwt} OW_w + ETC_{pwt} \quad \forall p, w, t \quad (23)$$

$$ETC_{pwt} \leq RT3_{pwt} CapT_{pwt} OW_w \quad \forall p, w, t \quad (24)$$

$$TAE_{pwt} = \sum_{mr_2 k} TA2_{pmwr_2 kt_p} - \sum_{cr_3 k} x_{pwcr_3 kt} \quad \forall p, w, t, t_p \Big| t_p = t - EX_p \quad (25)$$

$$x_{pwcr_3 kt} = \sum_{tp} TA3_{pwcr_3 kt_p} \quad \forall p, w, c, r_3, k, t, t_p \Big| t_p < t, t - t_p < EX_p \quad (26)$$

$$\sum_{ip} IL2_{ipmt} \leq (1 - RH_{mt}) CapH_{mt} OM_m \quad \forall m, t \quad (27)$$

$$\sum_p IL1_{pwt} \leq (1 - RH_{wt}) CapH_{wt} OW_w \quad \forall w, t \quad (28)$$

$$IL1_{ipmt} = IL1_{ipm(t-1)} + \sum_{sr_1 k} TA1_{ismr_1 kt} - \frac{PA_{pmt}}{\delta_ip} \quad \forall i, p, m, t \quad (29)$$

$$\frac{PA_{pmt}}{\delta_ip} \leq IL2_{ipm(t-1)} - \sum_{sr_1 k} TA1_{ismr_1 kt} \quad \forall i, p, m, t \quad (30)$$

$$PA_{pmt} \leq (1 - RP_{pmt}) CapP_{pmt} OM_m \quad \forall p, m, t \quad (31)$$

$$IL_{pwt} = IL_{pw(t-1)} + \sum_{mr_2 k} TA2_{pmwr_2 kt_p} - TAE_{pwt} - \sum_{cr_3 k} TA3_{pwcr_3 kt} \quad \forall p, w, t, t_p \Big| t_p < t, t - t_p < EX_p \quad (32)$$

$$\sum_{mr_2 k} TA2_{pmwr_2 kt_p} = (1 - Re_{pmt}) PA_{pmt} \quad \forall p, m, t \quad (33)$$

$$\sum_p TA1_{ismr_1 kt} \leq SM_{ismr_1 kt} BM \quad \forall i, s, m, r_1, k, t \quad (34)$$

$$TA2_{pmwr_2 kt} \leq MW_{pmwr_2 kt} BM \quad \forall p, m, w, r_2, k, t \quad (35)$$

$$TA3_{pwcr_3 kt} \leq WC_{pwcr_3 kt} BM \quad \forall p, w, c, r_3, k, t \quad (36)$$

$$\sum_{wrs k} TA3_{pwcr_3 kt} + LS_{pct} = De_{pc(t-1)} + LS_{pc(t-1)} \quad \forall p, c, t \quad (37)$$

$$\sum_{cr_3 k} TA3_{pwcr_3 kt} \leq \sum_{mr_2 k} TA2_{pmwr_2 kt} + IL_{pw(t-1)} - TAE_{pwt} \quad \forall p, w, t \quad (38)$$

$$\frac{TA2_{pmwr_2kt}}{\rho_p} = z_{pmwr_2kt} \quad \forall p, m, w, r2, k, t \quad (39)$$

$$\sum_p z_{pmwr_2kt} \leq CapZ_k \quad \forall m, w, r2, k, t \quad (40)$$

$$\sum_{ip} TA1_{ipsmr_1kt} \leq CapV_k \quad \forall s, m, r1, k, t \quad (41)$$

$$\sum_p TA2_{pmwr_2kt} \leq CapV_k \quad \forall m, w, r2, k, t \quad (42)$$

$$\sum_p TA3_{pwcr_3kt} \leq CapV_k \quad \forall w, c, r3, k, t \quad (43)$$

$$CS_s = 1 | \sum_{ipmr_1kt} TA1_{ipsmr_1kt} \geq \tau_s \quad \forall s \quad (44)$$

$$CM_m = 1 | \sum_{ipsr_1kt} TA1_{ipsmr_1kt} + \sum_{pwr_2kt} TA2_{pmwr_2kt} + \sum_{ipt} \frac{PA_{pmt}}{\delta_{ip}} + \sum_{ip} IL1_{ipm(nt|nt=t)} \\ \geq \tau_m \quad \forall m \quad (45)$$

$$CW_w = 1 | \sum_{pmr_2kt} TA2_{pmwr_2kt} + \sum_{pcr_3kt} TA3_{pwcr_3kt} + \sum_{pt} IL2_{wpt} + \sum_{pt} TAE_{pwt} \\ \geq \tau_w \quad \forall w \quad (46)$$

$$\sum_{ipsmr_1k} TA1_{ipsmr_1kt} + \sum_{pmwr_2k} TA2_{pmwr_2kt} + \sum_{pwcr_3k} TA3_{pwcr_3kt} \leq \sum_k CapV_k \quad \forall t \quad (47)$$

$$\sum_{smpr_1} SM_{smpr_1kt} + \sum_{mwpr_2} MW_{mwpr_2kt} + \sum_{wcpr_3} WC_{wcpr_3kt} \leq 1 \quad \forall k, t \quad (48)$$

$$OS_s, OM_m, OW_w, CS_s, CM_m, CW_w, SM_{ismr_1kt}, MW_{pmwr_2kt}, WC_{pwcr_3kt} \in \{0, 1\} \quad (49)$$

$$TFOC, TTC, TDC, TOC, TBC, THC, TSHC, TECC, TAE_{pwt}, x_{pwcr_3kt}, IL1_{ipmt} \\ , IL2_{pwt}, TA1_{ipsmr_1kt}, ETC_{ist} \geq 0 \quad (50)$$

$$LS_{pct}, z_{pmwr_2kt}, TA2_{pmwr_2kt}, TA3_{pwcr_3kt}, ETC_{pmt}, ETC_{pwt} \in int \quad (51)$$

The mathematical model has two objective functions. The first objective function, Eq. (1) minimizes the total costs of the SC, while the second objective function, Eq. (2) minimizes the critical points and the number of allocations. The costs of construction, purchase, transportation, distribution, manufacturing, backlog sales, maintenance, and excess transportation are calculated in Constraints (3) to (10), respectively. Constraints (11) to (13) are related to allocation, indicating that each point is connected to only one other point in its upper or lower echelons. Constraints (14) to (18) are related to route disruptions, indicating that it will not be possible to connect echelons from a disrupted route. Constraints (19), (21) and (23) control the capacity and excess capacity of transport routes. Constraints (20), (22) and (24) calculate the excess transport capacity. Constraints (25) and (26) calculate the volume of spoiled goods within the SC. Constraints (27) and (28) limit the inventory level of warehouses. Constraint (29) is an equilibrium constraint between the first and second echelons that regulates the inventory level of raw materials. Constraint (30) shows that the manufacturing of a new product requires the presence of raw materials. Constraint (31) controls the manufacturing ratio of the new product to the production capacity of the manufacturer. Constraint (32) is an equilibrium constraint between the second and third echelons that adjusts the inventory level of the distributor's warehouse. Constraint (33) specifies that all healthy products can be transported to distributors' warehouses. Constraints (34), (35), and (36) state that inter-

echelon transportation is possible only if there is allocation. Constraint (37) ensures that the demand of retailers and backlog sales in the previous periods equals the volume of distributed products and backlog sales in this period. Constraint (38) is an equilibrium constraint stating that the volume distributed by the distributor is always smaller than the inventory of the distributor at the end of the previous period and the volume of incoming products in this period after the deduction of the spoiled products. Constraint (39) calculates the number of products in each package. Constraints (40), (41), (42) and (43) control the weight and number of vehicles. Constraints (44), (45), and (46) determine the critical points of the SC. Constraint (47) states that the total volume transported in each period is at most equal to the total capacity of vehicles. Constraint (48) ensures that each vehicle can only move between two echelons during each period. Constraints (49–51) define binary, positive, and integer variables. In this model, first, some constraints are non-linear. To deal with this problem, they have to be linearized. Second, operational risks have a negative impact on the model due to the inherent uncertainties in the parameters and fluctuations in the business environment. We need a systematic procedure to encounter such threats. Third, risks are applied to the SC due to the uncertainty in the retailers' demand. Thus, we need a systematic approach to counter these threats. Fourth, the proposed formula consists of several objective functions. Therefore, multi-objective programming techniques should be used to deal with this problem.

3.2. Model linearization

Constraints (44), (45), and (46) are non-linear, so we replace them with the following linear constraints in order to linearize them.

$$\sum_{ipmr_1kt} TA1_{ipsmr_1kt} \leq BM.CS_s + \tau_s \quad \forall s \quad (52)$$

$$\sum_{ipmr_1kt} TA1_{ipsmr_1kt} > CS_s \cdot \tau_s \quad \forall s \quad (53)$$

$$\sum_{ipsr_1kt} TA1_{ipsmr_1kt} + \sum_{pwr_2kt} TA2_{pmwr_2kt} + \sum_{ipt} \frac{PA_{pmt}}{\delta_{ip}} + \sum_{ip} IL1_{ipm(nt|nt=t)} \\ \leq BM.CM_m + \tau_m \quad \forall m \quad (54)$$

$$\sum_{ipsr_1kt} TA1_{ipsmr_1kt} + \sum_{pwr_2kt} TA2_{pmwr_2kt} + \sum_{ipt} \frac{PA_{pmt}}{\delta_{ip}} + \sum_{ip} IL1_{ipm(nt|nt=t)} \\ > CM_m \cdot \tau_m \quad \forall m \quad (55)$$

$$\sum_{pmr_2kt} TA2_{pmwr_2kt} + \sum_{pcr_3kt} TA3_{pwcr_3kt} + \sum_{pt} IL2_{wpt} + \sum_{pt} TAE_{pwt} \\ \leq BM.CW_w + \tau_w \quad \forall w \quad (56)$$

$$\sum_{pmr_2kt} TA2_{pmwr_2kt} + \sum_{pcr_3kt} TA3_{pwcr_3kt} + \sum_{pt} IL2_{wpt} + \sum_{pt} TAE_{pwt} > CW_w \cdot \tau_w \quad \forall w \\ (57)$$

3.3. Stochastic programming approach

In the two-stage programming method, a stochastic linear problem is converted into an equivalent deterministic problem.

For uncertain parameters ϑ

Support Set : u

a PDF(Probability Distribution Function) Of ϑ on $u : \gamma$

$$P : u \rightarrow R : \gamma_\vartheta \in [0, 1] \quad \forall \vartheta \in u, \int_{\vartheta \in u} \gamma_\vartheta d_\vartheta = 1 \quad (58)$$

$$\min_{x \in X} c^T x + E_P[x; \vartheta]$$

As a result, to eliminate the uncertainty present in the disruptions of the paths, the first objective function is developed as follows. All parameters and variables related to the path are indexed by 'o'.

$$\min \text{cost} = \text{TFOC}$$

$$+ \sum_o \pi_o (\text{TBC}_{\text{o}} + \text{TOC}_{\text{o}} + \text{TTC}_{\text{o}} + \text{TDC}_{\text{o}} + \text{THC}_{\text{o}} + \text{TSHC}_{\text{o}} + \text{TECC}_{\text{o}}) \quad (59)$$

3.4. Robust data-driven planning approach

In this approach, the stochastic linear problem is formulated as a distributionally robust optimization (DRO) model and then transformed into an equivalent deterministic counterpart: a family of probability distributions is constructed over the uncertainty support, the worst-case distribution is selected from a distance-based ambiguity set, and the resulting inner maximization is reformulated to produce a deterministic robust counterpart.

Algorithm 1

DRO formulation

- Uncertain parameter and support:** let θ denote uncertain parameters with finite support u , $|u| = S$; index the scenario set $\Xi = \{1, 2, \dots, S\}$ and write $\theta_{\xi} \in u$ in u for $\xi \in \Xi$. Define $\pi_{\xi} = p_{\theta_{\xi}}$ and $P = [\pi_1, \dots, \pi_S]^T$ with $1^T P = 1$.
- DRO problem:** the data-driven distributionally robust optimization problem is formulated as $\text{DRO} = \min_{x \in X} C^T x + \max_{p \in P} E_p[g(x, \theta)] = \min_{x \in X} C^T x + \max_{p \in P} p^T g(x, \theta)$ (60) where $X = \{x \in R^N | kx \leq h\}$ and $g(x, \theta)$ is the scenario-wise second-stage cost vector (size S).
- Ambiguity (distance-based) set:** the ambiguity set is defined around a nominal empirical distribution $p = \{P = P^0 + G \in M_+(u) | 1^T G = 0, -\psi^l P^0 \leq G \leq \psi^u (1 - P^0)\}$ (61) where P^0 is the nominal distribution ($1^T G = 0$), G is the perturbation, and $0 \leq \psi^u \leq 1$ and $0 \leq \psi^l \leq 1$, control allowable downward/upward deviations.
- Inner maximization and linearization:** substituting $P = P^0 + G$ yields the inner maximization $\max_{p \in P} p^T g(x, \theta) = \max_{p \in P} (P^0 + G)^T g(x, \theta)$ subject to $1^T G = 0$ and $-G\psi^l P^0 \leq G \leq \psi^u (1 - P^0)$. The maximization over G is a linear program with linear bounds and is therefore tractable and dualizable.
- Deterministic reformulation via dualization:** dualizing the inner LP and combining with the outer minimization gives the deterministic reformulation $\text{DRO} = \min_{x, \lambda, \nu, \nu} C^T x + P^0^T g(x, \theta) + \psi^u (1 - P^0)^T v + \psi^l P^0^T \nu$ (62) with $g(x, \theta) = \min_{w \in W} g^T w$ and $W = \{w \in R^M | b - Dx\}$ in which $\lambda + \nu + v = g(x, \theta)$, $\lambda \in R$, $\nu \in R_+^S$, and $v \in R_+^S$.

After this reformulation the uncertain problem becomes a deterministic mixed-integer program suitable for standard MIP solvers.

3.5. Stochastic model

According to the explanations above, the final model of the problem is as follows.

$$\min z_1 = \min \text{cost}$$

$$= \text{TFOC} + \sum_u \beta_u \sum_o \pi_o (\text{TBC}_{\text{o}} + \text{TOC}_{\text{o}} + \text{TTC}_{\text{o}} + \text{TDC}_{\text{o}} + \text{THC}_{\text{o}} + \text{TSHC}_{\text{o}} + \text{TECC}_{\text{o}}) \\ + \text{TSHC}_{\text{o}} + \text{TECC}_{\text{o}}) + \psi_{\text{upper}} * \sum_u (1 - \beta_u) \eta_u + \psi_{\text{lower}} * \sum_u \beta_u v_u \quad (63)$$

$$\min z_2 = TN$$

$$= \sum_s \varphi_1 OS_s + \sum_m \varphi_2 OM_m + \sum_w \varphi_3 OW_w + \sum_s \theta_1 CS_s + \sum_m \theta_2 CM_m \\ + \sum_w \theta_3 CW_w + \sum_{smr_1ktou} \mu_1 SM_{smr_1ktou} + \sum_{smr_1ktou} \mu_2 MW_{smr_1ktou} \\ + \sum_{smr_1ktou} \mu_3 WC_{smr_1ktou} \quad (64)$$

$$\text{TFOC} = \sum_s EC_s OS_s + \sum_m EC_m OM_m + \sum_w EC_w OW_w \quad (65)$$

$$\text{TBC}_{\text{o}} = \sum_{ipsmr_1kt} TA1_{ipsmr_1kt} B_i \quad \forall o, u \quad (66)$$

$$\begin{aligned} \text{TCC}_{\text{o}} &= \sum_{ipsmr_1kt} TA1_{ipsmr_1kt} TC1_{r_1kt} ds_{smr_1} \\ &+ \sum_{pmwr_2kt} TA2_{pmwr_2kt} TC2_{r_2kt} dm_{mwr_2} \quad \forall o, u \end{aligned} \quad (67)$$

$$\text{TDC}_{\text{o}} = \sum_{pwcr_3kt} TA3_{pwcr_3kt} DC_{r_3kt} dw_{wcr_3} \quad \forall o, u \quad (68)$$

$$\text{TOC}_{\text{o}} = \sum_{pmt} PC_{pmt} PA_{pmt} + \sum_{pmt} PCe_{pmt} RPA_{pmt} \quad \forall o, u \quad (69)$$

$$\text{TSHC}_{\text{o}} = \sum_{pctou} SC_{pctou} LS_{pctou} \quad \forall o, u \quad (70)$$

$$\begin{aligned} \text{THC}_{\text{o}} &= \sum_{ipmt} HC1_{ipmt} IL1_{ipmt} + \sum_{pwt} HC2_{pwt} IL2_{pwt} \\ &+ \sum_{pwt} ECe_{pwt} TAE_{pwt} \quad \forall o, u \end{aligned} \quad (71)$$

$$\begin{aligned} \text{TECC}_{\text{o}} &= \sum_{ist} VC1_{ist} ETC1_{ist} + \sum_{pmt} VC2_{pmt} ETC2_{pmt} \\ &+ \sum_{pwt} VC3_{pwt} ETC3_{pwt} \quad \forall o, u \end{aligned} \quad (72)$$

s.t. :

$$\sum_{r_1k} SM_{ismr_1kt} \leq 1 \quad \forall i, s, m, t, o, u \quad (73)$$

$$\sum_{r_2k} MW_{pmwr_2kt} \leq 1 \quad \forall p, m, w, t, o, u \quad (74)$$

$$\sum_{r_3k} WC_{wcr_3kt} \leq 1 \quad \forall w, c, t, o, u \quad (75)$$

$$\sum_{ik} SM_{ismr_1kt} \leq OS_s (1 - \omega_{smr_1tou}) \quad \forall s, m, r_1, t, o, u \quad (76)$$

$$\sum_{ik} SM_{ismr_1kt} \leq OM_m (1 - \omega_{smr_1tou}) \quad \forall s, m, r_1, t, o, u \quad (77)$$

$$\sum_{pk} MW_{pmwr_2kt} \leq OM_m (1 - \eta_{mwr_2tou}) \quad \forall m, w, r_2, t, o, u \quad (78)$$

$$\sum_{pk} MW_{pmwr_2kt} \leq OW_w (1 - \eta_{mwr_2tou}) \quad \forall m, w, r_2, t, o, u \quad (79)$$

$$\sum_k WC_{wcr_3kt} \leq OW_w (1 - \lambda_{wcr_3tou}) \quad \forall w, c, r_3, t, o, u \quad (80)$$

$$\sum_{smr_1k} TA1_{ipsmr_1kt} \leq (1 - RT1_{istou}) CapT_{ist} OS_s + ETC_{istou} \quad \forall i, s, t, o, u \quad (81)$$

$$ETC_{istou} \leq RT1_{istou} CapT_{ist} OS_s \quad \forall i, s, t, o, u \quad (82)$$

$$\sum_{wr_2k} TA2_{pmwr_2kt} \leq (1 - RT2_{pmtou}) CapT_{pmt} OM_m + ETC_{pmtou} \quad \forall p, m, t, o, u \quad (83)$$

$$ETC_{pmtou} \leq RT2_{pmtou} CapT_{pmt} OM_m \quad \forall p, m, t, o, u \quad (84)$$

$$\sum_{cr_3k} TA3_{pwcr_3ktou} \leq (1 - RT3_{pwtou}) CapT_{pwt} OW_w + ETC_{pwtou} \quad \forall p, w, t, o, u \quad (85)$$

$$ETC_{pwtou} \leq RT3_{pwtou} CapT_{pwt} OW_w \quad \forall p, w, t, o, u \quad (86)$$

$$TAE_{pwtou} = \sum_{mr_2k} TA2_{pmwrt_2ktou} - \sum_{cr_3k} x_{pwcr_3ktou} \quad \forall p, w, t, o, u | t_p = t - EX_p \quad (87)$$

$$x_{pwcr_3ktou} = \sum_{tp} TA3_{pwcr_3ktou} \quad \forall p, w, c, r, k, t, o, u, t_p \left| t_p < t, t - t_p < EX_p \right. \quad (88)$$

$$\sum_{ip} IL2_{ipmtou} \leq (1 - RH_{mtou}) CapH_{mt} OM_m \quad \forall m, t, o, u \quad (89)$$

$$\sum_p IL1_{pwtou} \leq (1 - RH_{wtou}) CapH_{wt} OW_w \quad \forall w, t, o, u \quad (90)$$

$$IL1_{ipmtou} = IL1_{ipm(t-1)ou} + \sum_{sr_1k} TA1_{ipsmr_1ktou} - \frac{PA_{pmtou}}{\delta_{ip}} \quad \forall i, p, m, t, o, u \quad (91)$$

$$\frac{PA_{pmtou}}{\delta_{ip}} \leq IL2_{ipm(t-1)ou} - \sum_{sr_1k} TA1_{ipsmr_1ktou} \quad \forall i, p, m, t, o, u \quad (92)$$

$$PA_{pmtou} \leq (1 - RP_{pmtou}) CapP_{pm} OM_m \quad \forall p, m, t, o, u \quad (93)$$

$$IL_{pwtou} = IL_{pw(t-1)ou} + \sum_{mr_2k} TA2_{pmwrt_2ktou} - TAE_{pwtou} \\ - \sum_{cr_3k} TA3_{pwcr_3ktou} \quad \forall p, w, t, o, u \quad (94)$$

$$\sum_{wr_2k} TA2_{pmwrt_2ktou} = (1 - Re_{pmtou}) PA_{pmtou} \quad \forall p, m, t, o, u, t_p \left| t_p < t, t - t_p < EX_p \right. \quad (95)$$

$$\sum_{ip} TA1_{ipsmr_1ktou} \leq SM_{smr_1ktou} BM \quad \forall s, m, r_1, k, t, o, u \quad (96)$$

$$\sum_p TA2_{pmwrt_2ktou} \leq MW_{mwrt_2ktou} BM \quad \forall m, w, r_2, k, t, o, u \quad (97)$$

$$\sum_p TA3_{pwcr_3ktou} \leq WC_{wcr_3ktou} BM \quad \forall w, c, r_3, k, t, o, u \quad (98)$$

$$\sum_{wr_3k} TA3_{pwcr_3ktou} + LS_{pctou} = De_{pc(t-1)ou} + LS_{pc(t-1)ou} \quad \forall p, c, t, o, u \quad (99)$$

$$\sum_{cr_3k} TA3_{pwcr_3ktou} \leq \sum_{mr_2k} TA2_{pmwrt_2ktou} + IL_{pw(t-1)ou} - TAE_{pwtou} \quad \forall p, w, t, o, u \quad (100)$$

$$\frac{TA2_{pmwrt_2ktou}}{\rho_p} = z_{pmwrt_2ktou} \quad \forall p, m, w, r_2, k, t, o, u \quad (101)$$

$$\sum_p z_{pmwrt_2ktou} \leq CapZ_k \sum_p MW_{pmwrt_2ktou} \quad \forall m, w, r_2, k, t, o, u \quad (102)$$

$$\sum_{ip} z_{pmwrt_2ktou} \leq CapV_k \sum_{ip} SM_{smr_1ktou} \quad \forall s, m, r_1, k, t, o, u \quad (103)$$

$$\sum_p TA2_{pmwrt_2ktou} \leq CapV_k \sum_p MW_{pmwrt_2ktou} \quad \forall m, w, r_2, k, t, o, u \quad (104)$$

$$\sum_p TA3_{pwcr_3ktou} \leq CapV_k \sum_p WC_{pwcr_3ktou} \quad \forall w, c, r_3, k, t, o, u \quad (105)$$

$$\sum_{ipmr_1kt} TA1_{ipsmr_1ktou} \leq BM.CS_s + \tau_{sou} \quad \forall s, o, u \quad (106)$$

$$\sum_{ipmr_1kt} TA1_{ipsmr_1ktou} > CS_s \cdot \tau_{sou} \quad \forall s, o, u \quad (107)$$

$$\sum_{ipmr_1kt} TA1_{ipsmr_1ktou} + \sum_{pwr_2kt} TA2_{pmwrt_2ktou} + \sum_{ip} \frac{PA_{pmtou}}{\delta_{ip}} + \sum_{ip} IL1_{ipm(nt|nt=t)ou} \\ \leq BM.CM_m + \tau_{mou} \quad \forall m, o, u \quad (108)$$

$$\sum_{ipmr_1kt} TA1_{ipsmr_1ktou} + \sum_{pwr_2kt} TA2_{pmwrt_2ktou} + \sum_{ip} \frac{PA_{pmtou}}{\delta_{ip}} + \sum_{ip} IL1_{ipm(nt|nt=t)ou} \\ > CM_m \cdot \tau_{mou} \quad \forall m, o, u \quad (109)$$

$$\sum_{pwr_2kt} TA2_{pmwrt_2ktou} + \sum_{pcr_3kt} TA3_{pwcr_3ktou} + \sum_{pt} IL2_{wptou} + \sum_{pt} TAE_{pwtou} \\ \leq BM.CW_w + \tau_{won} \quad \forall w, o, u \quad (110)$$

$$\sum_{pwr_2kt} TA2_{pmwrt_2ktou} + \sum_{pcr_3kt} TA3_{pwcr_3ktou} + \sum_{pt} IL2_{wptou} + \sum_{pt} TAE_{pwtou} \\ > CW_w \cdot \tau_{won} \quad \forall w, o, u \quad (111)$$

$$\sum_{ipsmr_1k} TA1_{ipsmr_1ktou} + \sum_{pmwrt_2k} TA2_{pmwrt_2ktou} + \sum_{pwcr_3k} TA3_{pwcr_3ktou} \\ \leq \sum_k CapV_k \quad \forall t, o, u \quad (112)$$

$$\sum_{smpr_1} SM_{smr_1ktou} + \sum_{mwp_2} MW_{mwrt_2ktou} + \sum_{wcp_3} WC_{wcr_3ktou} \leq 1 \quad \forall k, t, o, u \quad (113)$$

$$\lambda + v_u - \nu_u = \sum_o \pi_o (TBC_{ou} + TOC_{ou} + TTC_{ou} + TDC_{ou} + THC_{ou} \\ + TSHC_{ou} + TECC_{ou}) \quad \forall u \quad (114)$$

$$OS_s, OM_m, OW_w, CS_s, CM_m, CW_w, SM_{smr_1ktou}, MW_{pmwrt_2ktou}, WC_{wcr_3ktou} \\ \in \{0, 1\} \quad (115)$$

$$TFOC_{ou}, TTC_{ou}, TDC_{ou}, TOC_{ou}, TBC_{ou}, THC_{ou}, TSHC_{ou}, TECC_{ou}, TAE_{pwtou}$$

$$x_{pwcr_3ktou}, IL1_{ipmtou}, IL2_{pwtou}, TA1_{ipsmr_1ktou}, ETC_{istou} \geq 0 \quad (116)$$

$$LS_{pctou}, z_{pmwrt_2ktou}, TA2_{pmwrt_2ktou}, TA3_{pwcr_3ktou}, ETC_{pmtou}, ETC_{pwtou} \in int \quad (117)$$

Given the complexity and multi-objective nature of the underlying model, and the exponential growth of solution time with instance size, we employ a two-stage solution protocol that combines an exact method and a metaheuristic. To leverage the complementary strengths of exact and heuristic approaches we adopt a two-stage solution protocol. For small, tractable instances we use the augmented ϵ -constraint method with an exact solver to produce reference Pareto points and to validate

the model and fitness computations. These exact solutions are then used to calibrate and benchmark a problem-specific NSGA-II implementation (parameter tuning, repair routines and hybrid local moves). Once validated, NSGA-II is applied to medium and large instances that are computationally infeasible for exact methods. This workflow preserves methodological rigor (through exact benchmarks), ensures scalability (through NSGA-II), and allows us to quantify the trade-off between optimality and computational effort via standard quality metrics and runtime comparisons reported in the experiments.

3.6. Augmented ϵ -constraint method

The AEC is a technique used to solve this category of problems. In this method, one of the objective functions remains the main objective function, and the other functions are transferred to the constraints. In this method, the solutions are sensitive to the epsilon parameter, so epsilon values should be defined for each objective function as $f_j^{\min} \leq \epsilon \leq f_j^{\max}$. In general, solving the problem using the AEC method involves a multi-step algorithm as follows:

Algorithm 2 Augmented ϵ -constraint (AEC) method

1. Calculation of the optimal values of individual objectives (values of other objectives will be achieved according to the solution obtained for the individual objective function);
2. Determining the minimum and maximum values of each objective in a table;
3. Converting the multi-objective problem into a single-objective problem; and
4. Obtaining the range of ϵ values from the table

In the classical ϵ -constraint (CEC) method, non-dominated solutions may also be selected as Pareto points. Therefore, the AEC approach was proposed as an appropriate approach to reduce the runtime and obtain appropriate Pareto solutions. The solution algorithm of this method is in accordance with the CEC method, with the difference that the objectives are prioritized in the first step using the lexicographic optimization method. Then, the objective function with a higher priority order is optimized. If the obtained solution is not efficient, the first objective function turns into a constraint, and the objective function with a lower priority order is optimized.

$$\begin{aligned} & \max f_i(x) \\ & \text{s.t.:} \\ & f_j(x) \geq \epsilon_j \quad j \neq i \\ & g(x) = b \quad x \geq 0 \end{aligned} \tag{118}$$

In the third step, the unequal constraint of the CEC method with variable excess or deficiency becomes an equal constraint. r_i is the range of the i th objective.

4. NSGA-II

Since problems involving earliness and tardiness belong to the class of NP-hard problems, the proposed problem in this study also falls into this category. Given that the solution time of NP-hard problems increases exponentially with problem size, the augmented ϵ -constraint method is employed to solve small-sized instances, while the NSGA-II metaheuristic algorithm is applied for medium- and large-sized instances. This approach not only ensures computational feasibility for larger problems but also allows for the evaluation of the accuracy and performance of the NSGA-II algorithm in comparison with exact methods. Both solution approaches are described in detail in the following sections. Considering the presence of two objective functions and the NP-Hard nature of the problem, we used the meta-heuristic NSGA-II to solve the model in large-size instances. This algorithm has

a faster solution in ranking and less computational complexity than the other methods, and it uses the crowding distance to obtain a more uniform solution front than other algorithms and to estimate the density of points surrounding the solutions. The general structure of the NSGA-II is as follows [32].

Algorithm 3

The pseudocode of the proposed algorithm

-
1. Create the initial population.
 2. Calculate the fitness criteria.
 3. Sort the population according to the dominance conditions.
 4. Calculate the crowding distance.
 5. Selection: As soon as the initial population is sorted based on the dominance conditions, its crowding distance value will be calculated, and the selection from among it will be started. This selection is based on two elements:
 - Population rank: Lower-rank populations are selected.
 - Distance calculation: Assuming that p and q are two members of the same rank, the member with a greater crowding distance is selected. Here, the selection priorities are rank and crowding distance.
 6. Perform crossover and mutation to generate new offspring.
 7. Combine the initial population and the population obtained from crossover and mutation.
 8. Replace the parent population with the best members of the population combined in the previous step: First, the lower-ranking members replace the previous parents, and then they are sorted according to the crowding distance. The initial population and the population resulting from crossover and mutation are first classified according to rank, and those with a lower rank are removed. Next, the remaining population is sorted according to the crowding distance. Here, sorting is carried out inside a front.
 9. Repeat all the steps until the stop condition is met.
-

The implementation details of the algorithm are as follows:

Selection operator: The roulette-wheel selection is employed to choose parents. The operator first computes each candidate's selection probability using the prescribed formula (with Beta denoting the selection parameter), then draws a uniform random number, and finally selects a parent by locating where that random number falls in the cumulative distribution of the computed probabilities.

$$P = \exp^{-\text{Beta} \cdot nPop} \tag{119}$$

Crossover operator: The uniform crossover operator is implemented to produce offspring each iteration by exchanging genes between two parent chromosomes (Parent 1 and Parent 2). A random binary mask is generated and, for each gene position, the mask determines the source parent: if the mask bit is 1 the gene is copied from Parent 1, otherwise it is copied from Parent 2. This mechanism transfers dispersed favorable genes effectively when advantageous traits are scattered across parent strands, making uniform crossover sometimes superior to other crossover methods. The process yields one or two offspring that are random yet structured combinations of parental genes, thereby enhancing population diversity and reducing the risk of premature convergence in the population [33]. The following example illustrates the crossover operator.

Parent 1	[1	1	1	1	0	0	1	0]
Parent 2	[0	1	0	0	1	1	0	1]
Random binary mask	[1	0	1	0	0	1	1	0]
Child 1	[1	1	1	0	1	0	1	1]
Child 2	[0	1	0	1	0	1	0	0]

Mutation operator: The Gaussian mutation operator is employed in this model. First, a mutation rate is defined that specifies the proportion of genes in each chromosome to be modified relative to the chromosome length. A binary mutation mask is then generated according to this rate, where each mask bit indicates whether the corresponding gene will undergo mutation. For genes marked for mutation, values are perturbed by adding Gaussian noise according to the prescribed equation. Genes subject to mutation are selected randomly using the binary mask, which

preserves stochastic diversity in the population and helps prevent premature convergence during the evolutionary process [33]. The Gaussian mutation formula is given by Eq. (120).

$$x_{new} = x + \delta(N(0, 1)) \quad (120)$$

where δ is the mutation strength (scale parameter) controlling the standard deviation of the Gaussian perturbation and $N(0, 1)$ is a standard normal random variable. In implementation, for each gene i flagged by the binary mutation mask we sample $\varepsilon_i \sim N(0, 1)$ and compute $x'_i = x_i + \delta \cdot \varepsilon_i$, then clip x'_i to the feasible interval $[0, 1]$ by $x'_i := \min(\max(x'_i, 0), 1)$. Finally, binarize with threshold $\theta : b_i = 1$ if $x'_i \geq \theta$, otherwise $b_i = 0$.

To clarify the operator, the following worked example is provided. In the example, we use $\delta = 0.3$ (equivalent to $\sigma = 0.3$ in the Gaussian noise) and $\theta = 0.5$. This formulation (masking, Gaussian perturbation scaled by δ , clipping, thresholding) preserves stochastic diversity while keeping genes within bounds.

Parent	[0 1 0 0 1 1 0 1]
Random binary mask	[0 1 1 0 0 1 0 1]
Mutated positions: 2, 3, 6, 8	
Sampled Gaussian noises: -0.40; +0.60; -0.80; -0.70	
Real-valued after clipping	[0.0 0.6 0.6 0.0 1.0 0.2 0.0 0.3]
Binary child ($\theta = 0.5$)	[0 1 1 0 1 0 0 0]

5. Computational results

In this section, we present the numerical results and validate the proposed model and algorithm. To this aim, we categorize the results into small and large size instances and analyze them. To validate the model presented in the previous section and evaluate the performance of the proposed algorithms, the parameters are first tuned, and several different-size instances are then solved. Their results are compared with those of the meta-heuristic MOPSO algorithm according to Ref. [34]. It should be noted that the problem under investigation includes the parameters of demand, manufacturing capacity, manufacturing costs, etc. The programs of this research were implemented by MATLAB 2021b and GAMs 24.1 using a computer with 8 GB RAM and Core i7 CPU.

5.1. Performance evaluation criteria

Multi-objective optimization methods approximate the Pareto optimal front with a set of non-dominated solutions. Making decisions about how to evaluate the quality of these solutions is important because the conflicting and incommensurable nature of some criteria complicates the process. Based on the [35], after normalizing the objective functions, the following metrics are used in this study.

- **Mean Ideal Distance (MID):** MID specifies the closeness between the Pareto solutions and the ideal point. The distance between the non-dominated solutions and the ideal point is calculated using this metric. The smaller its value, the higher the priority of the algorithm. It is calculated from the following equation:

$$MID = \frac{\sum_n \sqrt{\left(\frac{f_i^1 - f_{Best}^1}{f_{max}^1 - f_{min}^1} \right)^2 + \left(\frac{f_i^2 - f_{Best}^2}{f_{max}^2 - f_{min}^2} \right)^2}}{n} \quad (121)$$

Table 2
Parameter levels of the NSGA-II.

Parameter	First Level	Second Level	Third Level
Number of Iterations	50	80	100
Population Size	15	25	50
Crossover Rate	0.7	0.8	0.95
Mutation Rate	0.2	0.25	0.3
Selection	2	3	4

- **Spread of Non-dominance Solutions (SNS):** This method is used to increase the diversity of solutions [54]. The higher its value, the higher the priority of the algorithm.

$$SNS = \sqrt{\frac{\sum_n \left(MID - \sqrt{\left(\frac{f_i^1 - f_{Best}^1}{f_{max}^1 - f_{min}^1} \right)^2 + \left(\frac{f_i^2 - f_{Best}^2}{f_{max}^2 - f_{min}^2} \right)^2} \right)}{n - 1}}{(122)}}$$

- **Rate of Achievement to Objectives Simultaneously (RAS):** This metric looks for a balance in achieving each objective, and its value is calculated using the following equation. The smaller its value, the higher the priority of the algorithm.

$$RAS = \frac{\sum_n \left[\left| \frac{f_i^1 - f_{Best}^1}{f_{Best}^1} \right| + \left| \frac{f_i^2 - f_{Best}^2}{f_{Best}^2} \right| \right]}{n} \quad (123)$$

- **Dispersion Measure (DM):** This metric is used to calculate the dispersion level of the optimal Pareto front solutions resulting from the algorithm. The greater its value, the higher the priority of the algorithm.
- **NOP:** This metric counts the number of solutions in the Pareto layer.

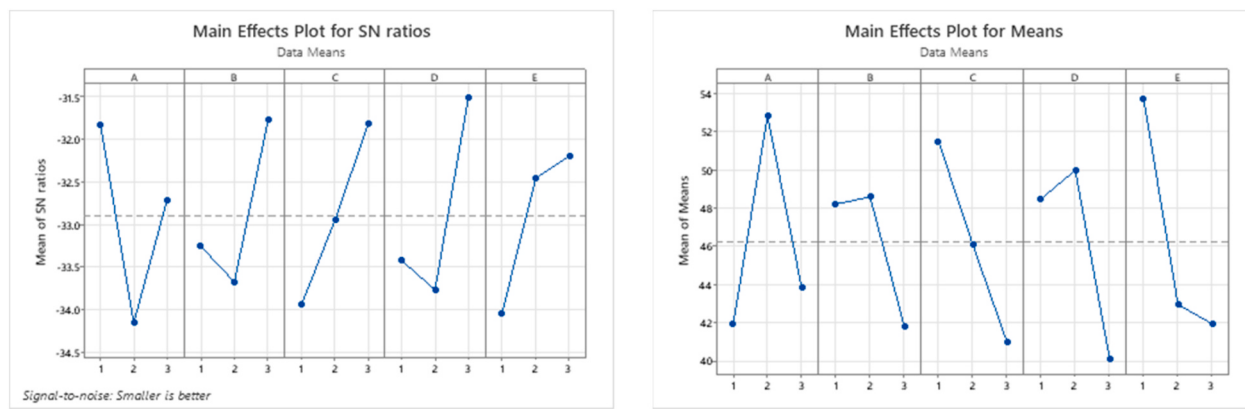
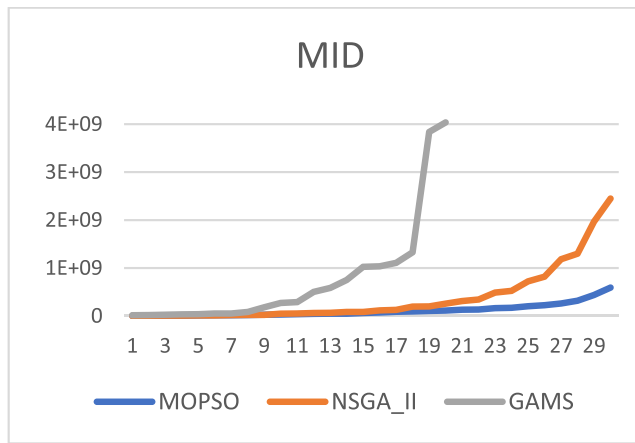
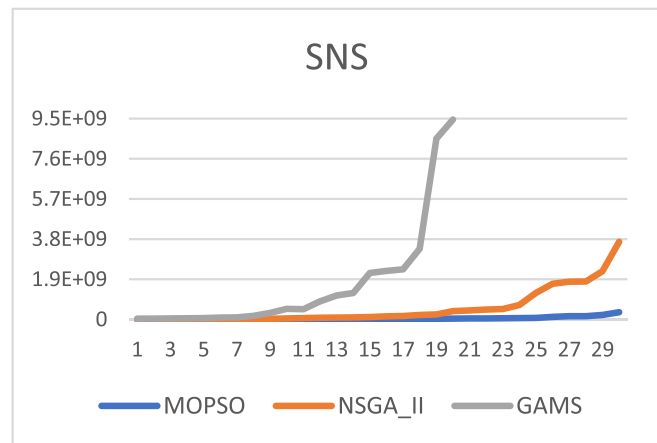
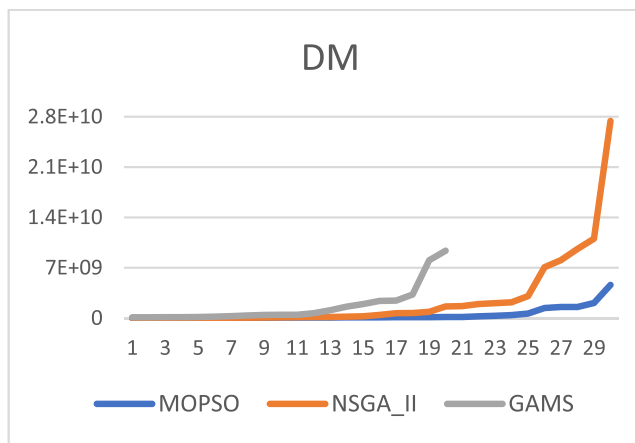
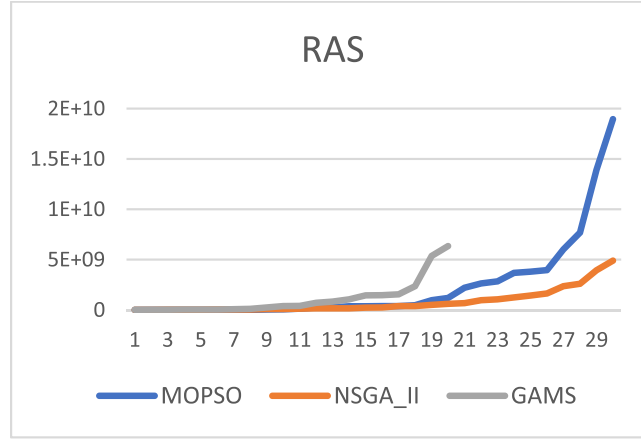
5.2. Parameters' tuning

Since the outputs of the problems are highly dependent on the parameters of the proposed algorithms, we use the Taguchi method to tune their parameters. The advantages of this method over the other experimental design methods lie in its cost-effectiveness as well as the capability of achieving the optimal levels of parameters within a shorter time. An important step in this method is the selection of an orthogonal array that estimates the effects of factors on the response mean and variations. In this study, the most suitable experimental design was a three-level experimental design. Based on Taguchi's standard orthogonal arrays, the L27 (3⁵) array was selected as a suitable experimental design to adjust the parameters of the proposed algorithms. In the Taguchi method, the optimal parameters are adjusted using a statistical measure of performance labeled as the signal-to-noise (S/N) ratio that takes both the mean and the variability into account. The higher this ratio at any level, the more favorable it is. The parameter levels of the NSGA-II are shown in Table 2.

Therefore, this algorithm is implemented as the number of Taguchi experiments to tune the parameters of the NSGA-II. After de-scaling the indices, the S/N ratios are calculated using the Minitab 21 software from the following formula.

$$RDI = \frac{|Method Sol - Best Sol| * 100}{|Max Sol - Min Sol|} \quad (124)$$

The results of parameter tuning using the Taguchi method are shown

**Fig. 2.** Parameters' tuning.**Fig. 3.** Comparisons in terms of MID.**Fig. 5.** Comparisons in terms of SNS.**Fig. 4.** Comparisons in terms of DM.**Fig. 6.** Comparisons in terms of RAS.

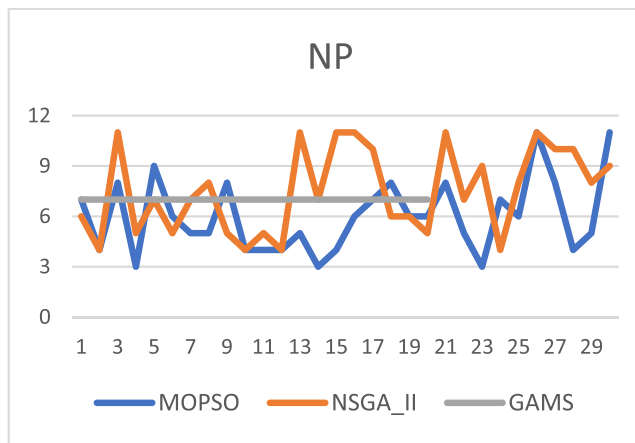


Fig. 7. Comparisons in terms of NP.

Table 3
Optimal values of the parameters.

Parameter	Value
Number of Iterations	50
Population Size	50
Crossover Rate	0.95
Mutation Rate	0.3
Selection	4

Table 4
The parameter values of instances.

Parameter	Value	Parameter	Value	Parameter	Value
φ_1	8	$CapT_{pwt}$	$[2.1, 3.9] \times 10^5$	τ_{sou}	$[1.4, 2] \times 10^4$
φ_2	7	RT_{istou}	$[0.2, 0.3]$	τ_{mou}	$[3.5, 6.5] \times 10^4$
φ_3	6	RT_{pmtou}	$[0.1, 0.3]$	τ_{wou}	$[3.5, 4.5] \times 10^4$
μ_1	5	RT_{pwto}	$[0.11, 0.21]$	π_o	$[0.2, 0.4]$
μ_2	4	EX_p	$[3.6, 12]$	β_u	$[0.3, 0.6]$
μ_3	3	Re_{pmtou}	$[0.05, 0.15]$	EC_s	$[8, 10] \times 10^4$
θ_1	12	RP_{pmtou}	$[0.02, 0.18]$	EC_m	$[6.5, 9.5] \times 10^4$
θ_2	11	RH_{mtou}	$[0.15, 0.25]$	EC_w	$[5.7] \times 10^4$
θ_3	10	RH_{wtou}	$[0.05, 0.35]$	$TC1_{r_1ktou}$	$[2.5, 12.5]$
ω_{smr_1to}	$[0, 1]$	$CapP_{pmt}$	$[7.3, 7.7] \times 10^7$	$TC2_{r_2ktou}$	$[2.5, 12.5]$
η_{mwr_2to}	$[0, 1]$	$CapH_{mt}$	$[1.95, 2.05] \times 10^8$	DC_{r_3ktou}	$[2.5, 12.5]$
λ_{wcr3to}	$[0, 1]$	$CapH_{wt}$	$[9.975, 1.0025] \times 10^8$	ds_{smr_1}	$[400, 800]$
$CapT_{ist}$	$[8.65, 9.35] \times 10^8$	δ_{ip}	$[15, 25]$	dm_{mwr_2}	$[250, 550]$
$CapT_{pmt}$	$[3.75, 4.25] \times 10^6$	De_{pctou}	$[1, 3] \times 10^5$	dw_{wcr_3}	$[50, 150]$
PC_{pmtou}	$[0.5, 3.5]$	VC_{istou}	$[7.5, 12.5]$	$CapZ_k$	$[800, 2200]$
PCE_{pmtou}	$[0.5, 3.5]$	VC_{pmtou}	$[6, 10]$	ρ_p	$[60, 200]$
ECE_{pwtou}	$[0.5, 2.5]$	VC_{pwtou}	$[3.8, 6.2]$	ψ^u	0.6
SC_{pctou}	$[80, 120]$	B_i	$[40, 60]$	ψ^l	0.4
$HC1_{imtou}$	$[1.5, 2.5]$	$CapV_k$	$[6000, 20000]$	$HC2_{pwtou}$	$[3, 5]$

in Fig. 2 and Table 3.

5.3. Numerical results

To compare the methods on the chosen metrics, thirty problem instances were randomly generated according to the parameter ranges in Table 4. Each instance was solved 15 times, and results were reported as the mean across runs. The baseline data and ranges were derived from an one-period dataset supplied by Khoshgovar Company, a producer and distributor of soft drinks. For this study, synthetic instances were generated by sampling around those baseline values to improve generalizability and enable controlled computational experiments.

Considering the validation metrics, it has outperformed the competing algorithm in the MID, DM, and SNS metrics in the small dimensions of the exact method as well as in the large dimensions of the NSGA-II. The results in small and large size instances are reported in Tables 5 and 6, respectively.

5.4. Analysis of results

This section presents graphs comparing the results of the algorithms according to the introduced criteria. It is known that the smaller the MID value is, the better it is. Therefore, as shown in Fig. 3, this metric is found to have a better value in the Multi-Objective Particle Swarm Optimization (MOPSO) method than in NSGA-II, and it is observed to have the lowest value in the exact method. Furthermore, considering DM, the exact method performs better in the dispersion index of Pareto front solutions in medium and small dimensions, while the NSGA-II performs better in large dimensions (see Fig. 4).

On the other hand, according to Fig. 5, the larger the SNS value, the better. Thus, the exact method has better performance in medium- and low-dimensional problems, whereas the NSGA-II performs in high-dimensional ones. Also, as demonstrated in Fig. 6, the lower the RAS value of a method, the better the method is. Therefore, the NSGA-II performs better than the other methods in this metric.

One of the metrics used to compare solution methods is the NP metric. The higher the value of this metric, the better the method is. However, it should be noted that this metric by itself cannot indicate which of the methods is superior because all the non-dominated solutions may fall within a certain range in a given method. Therefore, this metric should be evaluated along with the dispersion index. Nevertheless, Fig. 7 shows that there is a larger number of Pareto front solutions in the NSGA-II method than in the other methods. Considering the dispersion index, we can say that the exact method performs better in medium- and low-dimensional problems, whereas the NSGA-II does so in high-dimensional ones. An important metric used to evaluate the best solution method is the runtime metric. In the above problem, the exact method has so much complexity and runtime of the model in medium- and high-dimensional problems that the processor is not able to continue the solving process. However, as shown in Fig. 8, the MOPSO method generally performs better than the NSGA-II in the runtime metric.

5.5. Sensitivity analysis

This section presents a sensitivity analysis. Because distributional uncertainty is the primary driver of conservatism in DRO and produces the largest, most interpretable effects on both solution structure and total cost, the analysis concentrates on uncertainty-related parameters. Figs. 9 and 10 show a clear, monotonic increase in both minimum cost and computational complexity as the level of distributional uncertainty rises. Mechanistically, enlarging the DRO ambiguity set forces more

Table 5

Numerical results in small-size instances.

No.	Runtime (s)	NP	RAS	SNS	DM	MID
1	1760	7	21142280	35167130	104649000	14949850
2	1570	7	27016094	41538993	107472741	20125792
3	2436	7	35550808	48599526	125674681	25138210
4	3618	7	45457694	55302170	134623790	32143460
5	3698	7	46756912	61249484	160733434	35371641
6	3574	7	50023046	87167025	188888374	50596209
7	5586	7	71553816	96779764	267044499	52393300
8	6947	7	117070299	167604330	366753100	82781205
9	28680	7	255906472	309751273	439256594	180953257
10	28630	7	381713120	500297454	461291132	269911985
11	69430	7	411134484	482781005	464256489	290716147
12	100236	7	710427805	852884234	666600496	502348409
13	110543	7	827376772	1131457312	1084862979	585043719
14	147340	7	1060829202	1252130742	1596248147	750119545
15	194900	7	1447058822	2200088853	1941757163	1023226781
16	200540	7	1463984836	2293749273	2394676354	1035238741
17	220320	7	1563849263	2373589833	2437471923	1106754238
18	250070	7	2356479304	3346657384	3283619373	1326683021
19	742900	7	5368488727	8552377352	8026536728	3837654923
20	779800	7	6346376779	9453772947	9364527352	4035845193

Table 6

Numerical results in large-size instances.

No.	MOPSO						NSGA-II					
	Runtime (s)	NP	RAS	SNS	DM	MID	Runtime (s)	NP	RAS	SNS	DM	MID
1	274	7	2269248	195542	3997533	2087471	629	6	9375711	840866	9380064	1507147
2	329	4	2809720	225497	4382853	3072172	679	4	12478710	7558632	10769300	4687656
3	738	8	3405102	365373	8153461	6953452	789	11	20242980	10785745	12516520	6239357
4	820	3	4175120	499943	12174859	7312588	799	5	25654880	13826950	16085420	8535153
5	898	9	4906898	569308	13140376	9903313	879	7	30142940	14901600	21364760	10121490
6	920	6	6625181	671035	15617016	13823640	1093	5	38406500	17324560	30924420	12827440
7	924	5	12647293	1066195	18321880	14849989	1448	7	41470610	20679670	41647720	19203250
8	1008	5	14425956	1298720	19781736	20306218	1560	8	47227114	30770910	62223850	20735310
9	2324	8	49860088	4969780	45165612	25333498	3157	5	95311460	30922960	86204312	23597115
10	3168	4	53548260	5414881	70021537	29584968	3370	4	101967470	45963467	107570600	47655730
11	6779	4	136208696	9315225	76699931	38442544	9653	5	132589973	60950300	128869293	50950404
12	11625	4	255443458	9527474	80964424	42674122	26821	4	164482900	75512914	143839424	62657246
13	14453	5	267348257	9965230	83889403	45924260	28610	11	165086150	84080632	145151700	66251667
14	18926	3	367395607	10305730	97158678	48061091	35762	7	170814734	95648143	194889934	82241430
15	21969	4	378203475	13414501	97668399	60724141	42485	11	232105329	108600200	245523100	82489112
16	23034	6	380392381	18494915	100674301	71445662	43425	11	250357200	141470440	448534355	115976822
17	30596	7	392984944	19280967	114970735	86382896	45776	10	387442200	159671949	670133550	125178600
18	37815	8	469426273	19577164	120853558	94694474	57376	6	396485545	208933523	702521856	193721100
19	76721	6	972878888	30108883	121602562	103879219	136593	6	512107391	237036000	865017387	197975227
20	82944	6	1191409284	35551043	141353190	112720876	156461	5	618635327	395343087	1611799416	255886299
21	227180	8	2207894369	42551861	161226736	132116523	360216	11	684837573	425174350	1667459647	309115370
22	270100	5	2643130997	49555175	251768257	134542735	466892	7	973990422	465833918	1951715299	341971216
23	281440	3	2851217972	56386554	319550906	163665872	490733	9	1050911243	493090876	2065480776	486358823
24	207360	7	3682715876	66370895	402968106	171565641	520733	4	1254785037	681717253	2202713000	525112101
25	269200	6	3798104962	67232406	635338292	202632910	618417	8	1443694679	1254561875	3060910953	720903824
26	311040	11	3961243997	118402712	1389875683	225461492	716100	11	1644125052	1685682288	7075952256	820988218
27	334600	8	6015220478	151997648	1535564813	260308379	817889	10	2366886809	1786653116	8050983673	1181896256
28	405760	4	7688511806	153507058	1536129119	317285100	872527	10	2600452000	1794859000	9622869160	1300225999
29	549200	5	13900141115	211574405	2105499702	437343415	886768	8	3936119839	2277467137	11033698830	1965487498
30	768000	11	18951285231	339773921	4609793409	591725523	906421	9	4901505356	3668291141	27401850019	2447549336

conservative solutions (larger reserves, additional contingency actions, and more scenario coverage). This additional conservatism increases the number of active decision variables and constraints, prolongs solve times, and raises the total-cost objective. The two plots therefore provide consistent evidence that greater uncertainty simultaneously worsens cost outcomes and increases model complexity. In fact, larger ambiguity radii admit more adverse distributions, which shift optimal policies

toward robustness at the expense of cost and solution simplicity.

This finding indicates that in dynamic and high-risk environments, achieving optimal decisions in supply chain management becomes increasingly challenging, requiring the use of more advanced computational algorithms and adaptive managerial strategies. The results clearly demonstrate the level of risk that companies and supply chain specialists should be prepared for in order to minimize total costs. By

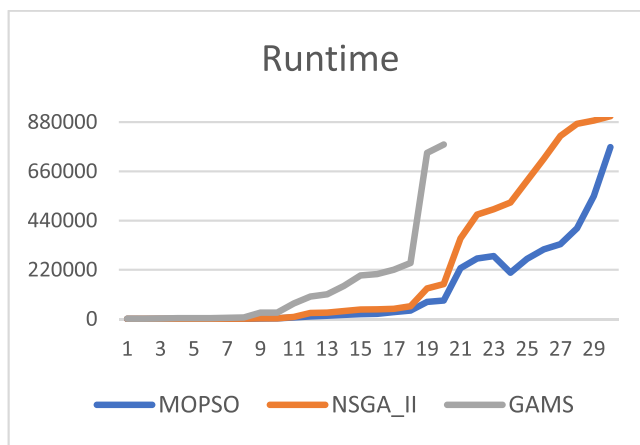


Fig. 8. Comparisons in terms of runtime.

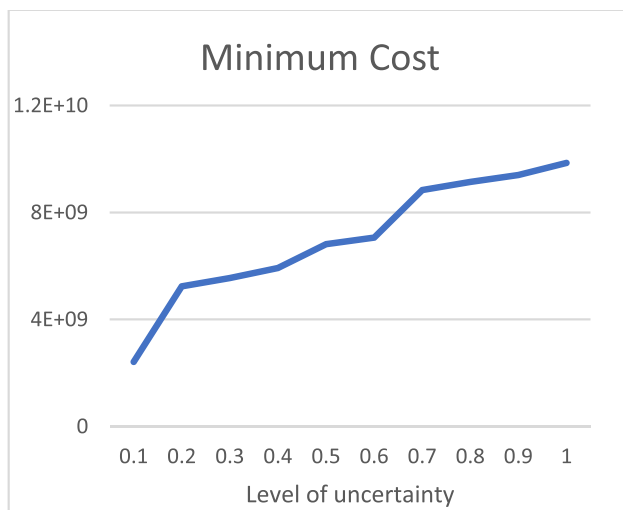


Fig. 9. Minimum cost vs. level of uncertainty.

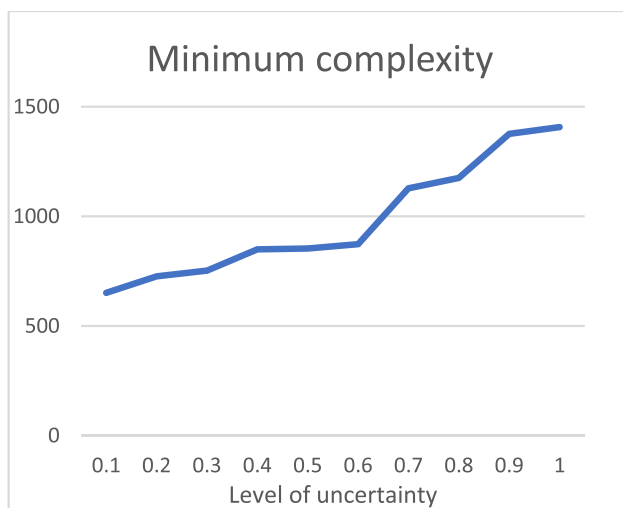


Fig. 10. Minimum complexity vs. level of uncertainty.

examining the impact of various uncertainty levels on supply chain performance, this study assists decision-makers in identifying an optimal balance between risk and cost. The significance of these findings lies in providing both practical and theoretical insights that enable managers to reduce operational expenses while maintaining resilience, stability, and efficiency within their supply chains. Therefore, the outcomes of this research can serve as an effective decision-support tool for designing and managing robust and efficient supply chains across different industries.

5.6. Managerial insights

This subsection distills actionable managerial insights with the explicit aim of translating empirical findings into operational guidance for designing resilient perishable-goods supply chains. Managers should note that both economic exposure and computational burden escalate rapidly with problem scale and uncertainty in the experiments. In the small instance set ([Table 5](#)), the RAS increases from 21,142,280 (instance 1) to 6,346,376,779 (instance 20), while runtimes rise from 1760 s (\approx 29.3 min) to 779,800 s (\approx 9.02 days). Comparable escalation appears in large instances ([Table 6](#)): MOPSO runtimes range from 274 s to 768,000 s and NSGA II runtimes range from 629 s to 906,421 s, with corresponding increases in NP, MID and other performance metrics. These results indicate a superlinear growth of cost exposure and solver effort as instance size and uncertainty increase, and they highlight a practical trade-off between solution diversity (NP, SNS/DM), MID, RAS, and computational feasibility (runtime). The following paragraphs summarize quantified takeaways, prescriptive recommendations, and short-term actions that managers may apply.

- **Quantified takeaways for managers:** The small-instance experiments report a roughly $300 \times$ increase in RAS (6,346,376,779/21,142,280 \approx 300) between instance 1 and instance 20 ([Table 5](#)). Runtimes in the same set grow from 1760 s (\approx 29.3 min) to 779,800 s (\approx 9.02 days). In the large-instance experiments ([Table 6](#)), MOPSO runtimes range from 274 s (No.1) to 768,000 s (No.30), and NSGA-II runtimes range from 629 s (No.1) to 906,421 s (No.30); these longer runs are accompanied by large absolute increases in RAS, MID and DM (for example, NSGA-II No.30: MID = 2,447,549,336 \approx 2.45 \times 10^9). Practically, when a single-instance runtime exceeds $O(10^4)$ seconds (\approx 2.78 h), exact solution procedures become impractical for routine planning; at that point metaheuristics such as NSGA-II provide feasible Pareto sets within operational deadlines. Under tight time constraints, prefer candidate fronts with lower MID (closer to the ideal) even when SNS/DM or NP are moderately smaller.
 - **Prescriptive recommendations for resilient perishable supply chains:** Given that distributional uncertainty is the dominant driver of DRO conservatism and given the measured escalation in cost and complexity, prioritise interventions that reduce uncertainty and increase operational flexibility. Specifically, allocate resources to improve short-horizon demand forecasting, integrate POS data, and strengthen supplier reliability metrics; these measures reduce the DRO ambiguity radius and thereby lower both expected cost and required contingency capacity. Operationally, prefer flexible sourcing, rapid replenishment options and contingency routing to permanently oversized inventory, because high-ambiguity solutions in [Tables 5 and 6](#) consistently correspond to substantially larger reserve requirements and higher total costs. Adopt a two-tier decision protocol: use exact or high-fidelity methods on representative small instances ([Table 5](#) rows, e.g., Nos. 1–8) to generate reference Pareto points and calibrate MID baselines, and deploy tuned metaheuristics ([Table 6](#) rows, e.g., NSGA-II Nos. 25–30) for routine, large-scale operational planning to produce timely, high-quality trade-offs.
 - **Concrete example recommendations for the next quarter:** If an operational problem matches the scale of [Table 5](#) entries 10–15 (runtimes \approx 28,630–194,900 s; RAS \approx 381,713,120–1,447,058,822),

switch weekly operational planning to a tuned NSGA-II implementation and reserve exact optimization for monthly calibration and benchmarking. For networks with high cost exposure, target a 10–20 % reduction in demand uncertainty through improved forecasting coordination and promotion alignment; the empirical tables show that even conservative uncertainty reductions at these scales will materially lower expected cost and required contingency capacity. Where solve times routinely exceed one day (runtime >86,400 s; **Table 5** Nos. 19–20 and **Table 6** higher-runtime rows), develop a calibrated NSGA-II configuration (population size, cross-over/mutation rates, repair routines) using small-instance exact fronts as benchmarks so that solutions are computationally feasible while remaining close to the ideal (low MID).

6. Conclusion and future studies

This paper develops a novel four-echelon, data-driven mixed-integer programming (MIP) model that integrates just-in-time (JIT) delivery requirements and resilience considerations for perishable-goods supply chains. The model explicitly captures stochastic retailer demand, fixed one-period delivery windows, backlog penalties, vehicle weight and volume limits, finite production and storage capacities, and disruption-prone transportation links. To manage distributional uncertainty, we adopt a distributionally robust optimization (DRO) approach that reduces sensitivity to ambiguous demand and disruption distributions. Given the problem's combinatorial complexity, we propose a scalable solution protocol that uses exact CPLEX solutions for small instances and the Non-dominated Sorting Genetic Algorithm II (NSGA-II) for large instances; performance is benchmarked against a Multi-Objective Particle Swarm Optimization (MOPSO) comparator. Computational experiments — conducted on datasets supplied by Khoshgavar Company (soft-drink production and distribution) — demonstrate the proposed framework's practical effectiveness: NSGA-II consistently provides superior Pareto fronts in terms of proximity to the ideal, dispersion, and objective attainment while enabling tractable solutions at realistic problem scales. Numerical results also quantify how cost exposure and computational burden escalate with instance size and ambiguity, motivating operational prescriptions such as prioritizing uncertainty reduction, investing in short-horizon forecasting and point-of-sale (POS) integration, and adopting a two-tier solution protocol (exact methods for calibration; metaheuristics for routine planning). The paper concludes with a concise discussion of model limitations and outlines directions for future work to enhance temporal dynamics, alternative ambiguity-set constructions, automated metaheuristic calibration, and industry case validation to translate Pareto outputs into deployable operational policies.

The model assumes fixed one-period delivery windows, complete manufacturer shipments each period, and single-period inventory at manufacturing sites; these simplifications limit applicability in contexts with variable delivery timing, partial shipments, or cross-period inventory dynamics. The DRO formulation, while data-driven, is restricted to the ambiguity-set constructions implemented here and does not exhaustively explore alternative uncertainty representations. Computationally, the study relies on metaheuristic calibration for scalability, which may require additional instance-specific tuning for deployment in heterogeneous industrial settings. Consideration for future extensions includes several promising directions: relaxing timing and shipment assumptions to permit variable delivery dates and partial or rolling shipments; extending the model to incorporate multi-period inventory management and explicit perishability dynamics; comparing alternative ambiguity-set constructions and estimating the marginal value of additional data for uncertainty reduction; and developing automated metaheuristic-calibration workflows alongside methods to translate Pareto outputs into compact, operational policies (for example, threshold rules) suitable for real-time use.

CRediT authorship contribution statement

Mohammad Mehdi Tahmouresi: Writing – original draft, Validation, Software, Investigation, Formal analysis, Data curation. **Javad Behnamian:** Writing – review & editing, Supervision, Methodology, Conceptualization.

Consent to participate

Not applicable.

Consent to publish

Not applicable.

Ethical approval

Not applicable.

Availability of data and materials

The datasets and codes used and/or analyzed in this study are available in the Figshare repository at <https://figshare.com/s/74e2809858b69275741a>; additional materials can be provided by the corresponding author upon reasonable request.

Funding

Not applicable.

Declaration of competing interest

The authors declare that they have no known competing financial interests or personal relationships that could have appeared to influence the work reported in this paper.

Data availability

The datasets and code used in this study are now available in the Figshare repository at <https://figshare.com/s/74e2809858b69275741a>.

References

- [1] Gao J, Zhang X, Zhong S. Privacy protection in steel supply chain via blockchain and attribute-based proxy re-encryption. *Array* 2025;28:100514.
- [2] Privett N, Gonsalvez D. The top ten global health supply chain issues: perspectives from the field. *Operations Research for Health Care* 2014;3(4):226–30.
- [3] Heizer J, Render B, Munson C. *Operations management: sustainability and supply chain management*. Pearson; 2020.
- [4] Christopher M, Peck H. Building the resilient supply chain. *Int J Logist Manag* 2004;15.
- [5] Sreedevi R, Saranga H. Uncertainty and supply chain risk: the moderating role of supply chain flexibility in risk mitigation. *Int J Prod Econ* 2017;193:332–42.
- [6] Pettit TJ, Fiksel J, Croxton KL. Ensuring supply chain resilience: development of a conceptual framework. *J Bus Logist* 2010;31(1):1–21.
- [7] Mahato S, Mahato F, Mahata GC. Game theoretical analysis in sustainable supply chain for perishable products incorporating transportation strategies and partial backlogging under carbon emissions. *J Clean Prod* 2025;519:145890.
- [8] Ye Y, Suleiman MA, Huo B. Impact of just-in-time (JIT) on supply chain disruption risk: the moderating role of supply chain centralization. *Ind Manag Data Syst* 2022;122(7):1665–85.
- [9] Vali-Siar MM, Roghanian E, Jabbarzadeh A. Resilient mixed open and closed-loop supply chain network design under operational and disruption risks considering competition: a case study. *Comput Ind Eng* 2022;172:108513.
- [10] Mousavi M, Jamali G, Ghorbanpour A. A green-resilient supply chain network optimization model in cement industries. *Industrial Management Journal* 2021;13(2):222–45.
- [11] Sadeghi Z, Boyer Hassani O. A multi-objective optimization model for the design and planning of sustainable and resilient supply chain at risk of supply disruption. *Journal of Engineering and Quality Management* 2019;3(9):212–25.

- [12] Mehralian G, Zarenezhad F, Rajabzadeh Ghatari A. Developing a model for an agile supply chain in pharmaceutical industry. *Int J Pharmaceut Healthc Market* 2015;9(1):74–91.
- [13] Zarenezhad Ashkezari F. Designing agile supply chain management in pharmaceutical industry of Iran (Master's thesis). University of Science and Culture; 2011 [In Persian].
- [14] Azad N, et al. Strategies for protecting supply chain networks against facility and transportation disruptions: an improved benders decomposition approach. *Ann Oper Res* 2013;210:125–63.
- [15] Garcia-Herreros P, Wassick JM, Grossmann IE. Design of resilient supply chains with risk of facility disruptions. *Ind Eng Chem Res* 2014;53(44):17240–51.
- [16] Nooraie SV, Parast MM. Mitigating supply chain disruptions through the assessment of trade-offs among risks, costs and investments in capabilities. *Int J Prod Econ* 2016;171:8–21.
- [17] Ghavamifar A, Makui A, Taleizadeh AA. Designing a resilient competitive supply chain network under disruption risks: a real-world application. *Transport Res E Logist Transport Rev* 2018;115:87–109.
- [18] Diabat A, Jabbarzadeh A, Khosrojerdi A. A perishable product supply chain network design problem with reliability and disruption considerations. *Int J Prod Econ* 2019;212:125–38.
- [19] Yan S, Ji X. Supply chain network design under the risk of uncertain disruptions. *Int J Prod Res* 2020;58(6):1724–40.
- [20] Dehghani Sadrabadi MH, Jafari-Nodoushan A, Bozorgi-Amiri A. Resilient supply chain under risks: a network and structural perspective. *Iran J Manag Stud* 2021;14(4):735–60.
- [21] Jafari-Nodoushan A, et al. Designing a sustainable disruption-oriented supply chain under joint pricing and resiliency considerations: a case study. *Comput Chem Eng* 2024;180:108481.
- [22] Khalili SM, Pooya A, Kazemi M, et al. Integrated resilient and sustainable gasoline supply chain model with operational and disruption risks: a case study of Iran. *Environ Dev Sustain* 2024. <https://doi.org/10.1007/s10668-024-05162-8>.
- [23] Karanam MK, Krishnanand L, Manupati VK. Quantifying performance indicators in perishable food supply chain networks: assessing dynamic performance under ripple effects. *Comput Ind Eng* 2025;201:110873.
- [24] Bakhshi Sasi M, Sarker RA, Essam DL. A novel heuristic algorithm for disruption mitigation in a global food supply chain. *Comput Ind Eng* 2024;194:110334.
- [25] Ansari F, Bozorgi-Amiri A, Shakibaei H. A data-driven multi-stage stochastic optimization for sustainable humanitarian supply chain using machine learning algorithms. *Eng Appl Artif Intell* 2025;161(Pt B):112133.
- [26] Hosseini Shekarabi S, Kiani Mavi R, Romero Macau F. An extended robust optimisation approach for sustainable and resilient supply chain network design: a case of perishable products. *Eng Appl Artif Intell* 2025;152:110846.
- [27] Tabatabaei SM. Sustainable supply chain network design: integrating risk management, resilient multimodal transportation, and production strategy. *Journal of Industrial Information Integration* 2025;47:100897.
- [28] Vázquez-Serrano JL, Cárdenas-Barrón LE, Vicencio-Ortiz JC, Smith NR, Bourguet-Díaz RE, Céspedes-Mota A, Peimbert-García RE. An integrated analytical framework for inventory and pricing of perishable products in multi-echelon supply chains. *Supply Chain Analytics* 2025;12:100157.
- [29] Lingkon MLR, Asadujjaman M, Dash A. An integrated model for freshness, cost reduction, and carbon footprint minimization of an efficient supply chain management for perishable goods. *Operations Research Forum* 2025;6:44. <https://doi.org/10.1007/s43069-025-00429-w>.
- [30] Rezki N, Mansouri M. Strategic supply chain network design: integrating risk management through mathematical modeling. In: Moldovan L, Gligor A, editors. *The 18th international conference interdisciplinarity in engineering, inter-eng 2024. Lecture notes in networks and systems, vol.1250*. Cham: Springer; 2025.
- [31] Hosseini Shekarabi S, Kiani Mavi R, Romero Macau F. Supply chain resilience: a critical review of risk mitigation, robust optimisation, and technological solutions and future research directions. *Global J Flex Syst Manag* 2025;26:681–735.
- [32] Coello CAC. *Evolutionary algorithms for solving multi-objective problems*. Springer; 2007.
- [33] Senthilkumar C, Ganeshan G, Karthikeyan R. Optimization of ECM process parameters using NSGA-II. *J Miner Mater Char Eng* 2012;11(10):931.
- [34] Komijani M, Sheikh Sajadieh M. An integrated planning approach for perishable goods with stochastic lifespan: production, inventory, and routing. *Cleaner Logistics and Supply Chain* 2024;12:100163.
- [35] Behnamian J, Fatemi Ghomi SMT, Zandieh M. A multi-phase covering Pareto-optimal front method to multi-objective scheduling in a realistic hybrid flowshop using a hybrid metaheuristic. *Expert Syst Appl* 2009;36(8):11057–69.